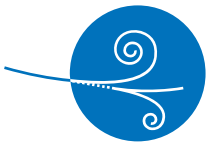

RWTH AACHEN UNIVERSITY

Master Thesis
Physics

Submitted to the III. Institute of Physics B at the
Faculty for Mathematics, Computer Science and Natural Science

RWTH AACHEN

Development of a Fast Betatron Tune and Chromaticity Measurement System Using Bunch-by-Bunch Position Monitoring

Philipp Niedermayer

Aachen, May 2021

Declaration of Authorship

I hereby declare that I have completed the present thesis independently and without illegitimate assistance from third parties. I have used no other than the specified sources and aids. In case that the thesis is additionally submitted in an electronic format, I declare that the written and electronic versions are fully identical. The thesis has not been submitted to any examination body in this or similar form.

(place, date)	(Philipp Niedermayer)

The thesis has been carried out under the supervision of:

1. Examiner:	**Prof. Dr. Andreas Lehrach**	(RWTH Aachen University)
2. Examiner:	**Prof. Dr. Anke Schmeink**	(RWTH Aachen University)
Supervisor:	**Dr. Bernd Breitkreutz**	(Forschungszentrum Jülich)

The thesis was prepared at the Nuclear Physics Institute (IKP-4) of
Forschungszentrum Jülich GmbH

Abstract

The betatron tune and its dependence on the momentum (chromaticity) are essential quantities of circular particle accelerators. The tune must be monitored in order to avoid optical resonances which cause instabilities and limit the lifetime of the stored particle beam. Control of the tune and chromaticity are also required to achieve long coherence times in spin polarization experiments as carried out by the JEDI collaboration.

In the scope of the present thesis, a fast betatron tune and chromaticity measurement system is developed for the Cooler Synchrotron COSY. The betatron oscillations of the beam are excited through stripline electrodes with a white noise RF signal in an appropriate frequency band. Resonant transverse oscillations are then observed using capacitive beam position monitors. Characteristic for the newly developed system is the determination of the betatron tune from bunch-by-bunch beam position measurements. This allows for time-discrete tune measurements within a few milliseconds as well as continuous tune monitoring – for example during the acceleration ramp.
The high precision tune measurement also enables determination of the beam chromaticity. Therefore, the beam momentum is varied by means of RF frequency sweeps and the subsequent tune change is measured. For routine use during beam operation and experiments, the developed method is integrated into the control system.
Finally, measurements showing the operational capabilities and limits of the method are presented. The influence of different parameters on the signal strength is analysed. For commissioning, control of the betatron tune and compensation of the chromaticity are demonstrated.

Kurzfassung

Der Betatron-Tune und seine Abhängigkeit vom Impuls (Chromatizität) sind zwei wesentliche Größen von Ring-Beschleunigern. Der Tune muss konstant überwacht werden, um optische Resonanzen zu vermeiden, welche Instabilitäten verursachen und die Lebensdauer des gespeicherten Teilchenstrahls begrenzen. Die korrekte Einstellung des Tunes und der Chromatizität ist außerdem essenziell, um lange Kohärenzzeiten in Spinpolarisations-Experimenten zu erreichen, wie sie von der JEDI-Kollaboration durchgeführt werden.

Im Rahmen der vorliegenden Arbeit wird ein schnelles Betatron-Tune- und Chromatizitätsmesssystem für das Kühler-Synchrotron COSY entwickelt. Dabei werden Betatronschwingungen des Strahls über Stripline-Elektroden mit einem HF-Signal weißen Rauschens in einem geeigneten Frequenzband angeregt. Die resonanten Transversalschwingungen werden mit kapazitiven Strahlpositionsmonitoren erfasst. Charakteristisch für das neu entwickelte System ist die Bestimmung des Betatron-Tunes aus den bunch-by-bunch Strahlpositionsmessungen. Damit ist eine zeitdiskrete Tune-Messung innerhalb weniger Millisekunden ebenso möglich wie eine kontinuierliche Überwachung des Tunes – beispielsweise während der Beschleunigungs-Rampe.
Die hochpräzise Tune-Messung ermöglicht außerdem die Bestimmung der Strahlchromatizität. Dazu wird der Strahlimpuls mittels der HF-Frequenz variiert und die damit einhergehende Tune-Änderung gemessen. Für den routinemäßigen Einsatz im Strahlbetrieb und bei Experimenten wird das neu entwickelte Verfahren in das Kontrollsystem integriert.
Abschließend werden Messungen vorgestellt, die die Einsatzmöglichkeiten und Grenzen der Methode zeigen. Der Einfluss verschiedener Parameter auf die Signalstärke wird analysiert und im Rahmen der Inbetriebnahme werden Steuerung des Betatron-Tunes und Kompensation der Chromatizität demonstriert.

Contents

Acronyms

ADC analog-to-digital converter
AFG arbitrary function generator
BBQ base-band tune
BPM beam position monitor
BTF beam transfer function
CA Channel Access
COSY Cooler Synchrotron
DFT discrete Fourier transform
EDM electric dipole moment
EPICS Experimental Physics and Industrial Control System
FAIR Facility for Antiproton and Ion Research
FESA Front-end Software Architecture
FFT fast Fourier transform
GSI GSI Helmholtz Centre for Heavy Ion Research
GUI graphical user interface
HBS High Brilliance Neutron Source
HESR High Energy Storage Ring
IKP Institut für Kernphysik (Nuclear Physics Institute)
IOC Input / Output Controller
JEDI Jülich Electric Dipole moment Investigations
JULIC Jülich Light Ion Cyclotron
LHC Large Hadron Collider
MAD Methodical Accelerator Design
PLL phase-locked loop
PV process variable
PWM pulse width modulation
PyDevSup Python Device Support
RF radio frequency
SM Standard Model of particle physics
STFT short-time Fourier transform

List of Symbols

Symbol	Physical quantity	Dimension	Page
D, $D(s)$	Dispersion	m	10
E, $E(t)$	Electric field	V/m	39
f_q	Betatron frequency	MHz	15
f_{rev}	Revolution frequency	MHz	11
k	Quadrupole strength	m^{-2}	5
p	Particle momentum	MeV/c	
P, $P(t)$	Signal power	W	39
Q	Tune		7
q	Fractional tune		7
R, $R(s)$	Radius of curvature	m	5
$r = f/f_{\mathrm{rev}}$	Relative frequency		26
s, x, y	Particle coordinates	m	5
$s_{\mathrm{max}} = L$	Orbit length (circumference)	m	
U, $U(t)$	Signal voltage	V	39
Z	Impedance	Ω	39
α_{p}	Momentum compaction factor		11
$\beta(s)$	betatron function	m	6
γ	Lorentz factor		
$\epsilon^{1\sigma}$	Beam emittance (1 sigma)	mm mrad	6
η	Slip factor		11
ξ	Total chromaticity		10
ξ_{nat}	Natural chromaticity		9
ξ/Q	Relative chromaticity		9
$\Psi(s)$	Phase advance	rad	6

List of Figures

List of Tables

1. Introduction

1.1. The Cooler Synchrotron COSY

The Nuclear Physics Institute (IKP) at Forschungszentrum Jülich [Ikp] operates the accelerator complex depicted in figure 1.1. Polarized or unpolarized particle beams are produced in an ion source and accelerated to an energy of 45 MeV in the Jülich Light Ion Cyclotron (JULIC). Besides being used for isotope production and studies at the low energy irradiation place, the ion beam can be injected into the Cooler Synchrotron (COSY). COSY is a storage ring with a circumference of 183.47 m, capable of accelerating proton and deuteron beams in the momentum range from 300 MeV/c up to 3.7 GeV/c [Die04; Cos]. Two electron cooling devices for the low and high energy range as well as a stochastic cooling system ensure excellent beam quality and long beam lifetimes. The beam can be stored and used for internal experiments, or it can be extracted to three external experimental areas.

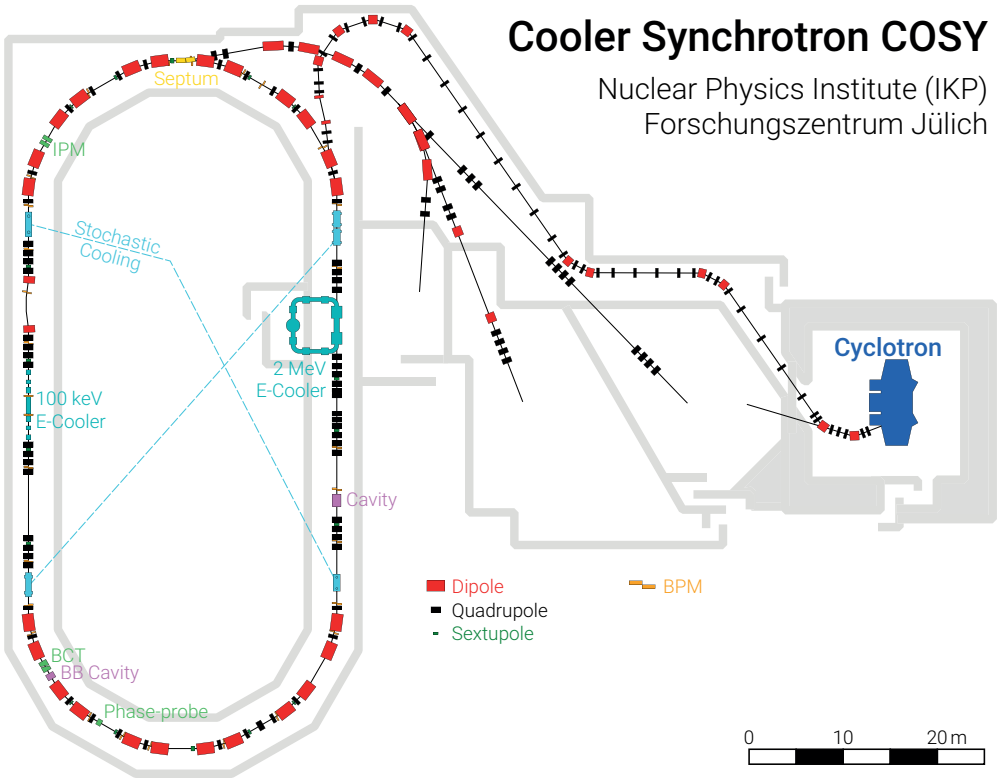

Figure 1.1.: Accelerator complex at the Nuclear Physics Institute (IKP)

The research and development at IKP focuses on three main activities [Geb20, p. 17]:

- Searches for an electric dipole moment (EDM) [Abu19].
- Construction of the High Energy Storage Ring (HESR) [Leh05], a proton and heavy ion accelerator being build for the future Facility for Antiproton and Ion Research (FAIR) at the GSI Helmholtz Centre for Heavy Ion Research (GSI).
- Activities towards the High Brilliance Neutron Source (HBS) [Brü20], a neutron research centre planned to provide neutron beams from a proton accelerator.

1.2. Searches for an electric dipole moment

The electric dipole moment (EDM) quantifies the separation of a particles charge along its principal axis. A subatomic particle with a *non-zero* permanent EDM would violate the time reversal symmetry (T). Violation of T is expected from the known violation of CP (charge and parity symmetry) in weak interactions according to the CPT-Theorem. However, a T-violating EDM has not been observed so far and only upper limits for its existence have been measured. [Gri04, pp. 134 sq.]
The Standard Model of particle physics (SM) predicts EDMs smaller than $10^{-31}\,e\,\mathrm{cm}$, which is orders of magnitude below the measured limits. Several theories have been proposed that predict higher values for the EDM near the current limits. A successful EDM measurement would therefore provide a test for physics beyond the SM. This would shine a light on challenging questions in modern physics: The matter–antimatter asymmetry of the universe can not be explained with the currently known CP violating processes. Furthermore, the observation of an oscillating EDM would support existing theoretical models for dark-matter candidates. [Abu19, pp. 1 sqq.]

The Jülich Electric Dipole moment Investigations (JEDI) collaboration aims to extend the existing limit on the EDM for protons and accomplish the first measurement for deuterons. Therefore, precursor experiments and EDM measurements on deuterons are carried out at COSY. These pave the way for a precision measurement of the proton EDM with a dedicated future storage ring. [Abu19; And20; Jed]
The storage ring is thereby used as a particle trap. Its magnetic and electric[1] fields act on the spin of the trapped particles according to the Thomas-BMT-Equation, causing the spin axis to precess. A non-vanishing EDM will cause the precession axis to tilt, producing a vertically oscillating spin component [Far04]. The EDM is then determined by measuring the vertical polarization built-up of a spin polarized beam. Since the oscillation is proportional to the very small EDM, a measurement time in the order of 15 min is required, during which the spin must stay coherent [Abu19, pp. 40 sqq.]. Therefore, one of the key requirements for such a measurement is to achieve a sufficiently long spin coherence time (polarization lifetime).

[1] In the particle rest frame the magnetic guiding fields produce motional electric fields $\vec{E} = \gamma\vec{v} \times \vec{B}$

1.3. Motivation and objective

Beam diagnostic is crucial for operation of an accelerator. The betatron tune (working point) and its dependence on the momentum (chromaticity) are two central quantities of interest – not only for the operating crew but also for experiments. They must be monitored to avoid resonances which cause beam instabilities and limit the lifetime of the stored particle beam.
For polarized beams additional intrinsic spin tune resonances also limit the polarization lifetime. To achieve sufficiently long spin coherence times, which are required for an EDM measurement as described in section 1.2, control of the tune and chromaticity is essential [Gui18]. This requires a precise measurement of these quantities multiple times per machine cycle.

The existing tune measurement system at COSY (tune sweep system) uses a beam transfer function measurement [Bre17]. With a measurement time of a few seconds, such a method is comparably slow by design and not capable of continuous tune tracking e.g. during the acceleration. A formerly used dynamic measurement system [Die98] has already reached the end of its life and can no longer be utilized.
The standard procedure for chromaticity measurements at COSY involves manual adjustment of the momentum and subsequent tune measurements over several machine cycles. This makes it a complex and time-consuming task not suited for routine monitoring and especially not for the systematic chromaticity scans envisaged by the JEDI collaboration.
Therefore, the need for a fast and automated tune and chromaticity measurement system arose, that is capable to fulfil the requirements by the operating crew and the JEDI collaboration.

In 2017 the beam position monitor (BPM) system of COSY was upgraded and new readout electronics were installed. These can measure the beam position of every particle bunch passing the BPM with a precision of 100 µm [Böh18; Kam19]. Already a few milliseconds of the bunch-by-bunch position data is in principle sufficient to determine the betatron tune.
Exploiting these capabilities, a fast and robust tune measurement system will be developed. The key requirements on the new system are:

- Measurement of the betatron tune for bunched beams
- Full beam energy range (45 MeV to 2.7 GeV)
- Measurement time below 100 ms
- Accuracy of 10^{-3} (or better)
- Multiple measurements per machine cycle

In addition, continuous measurements during the acceleration ramp are desired.

Based on the tune measurement an automated chromaticity measurement system will be developed. The key requirements are:

- Measurement of the *total* chromaticity taking the effect of sextupole magnets into account
- At least one, preferably three measurements per machine cycle
- Sensitive to values close to zero chromaticity

The tune and chromaticity measurement systems will be used by the JEDI collaboration in scope of precursor experiments carried out at COSY. Systematic measurements will be performed to study the dependence of the spin coherence time on the horizontal and vertical chromaticity and tune. Thereby the working point providing the longest possible spin coherence time can be found.

2. Theory of Accelerator Physics

2.1. Transverse linear beam dynamics

In particle accelerators, magnetic fields are used to guide the particle beam. While dipole fields bend the trajectory onto a closed orbit, quadrupole fields stabilize the particle motion by the effect of strong focussing [Hin08, pp. 180 sqq.]. The main purpose of sextupole fields is the chromaticity compensation described in section 2.1.5. In some facilities like the Large Hadron Collider (LHC) additional higher order fields are required to counteract field errors and improve beam operation.

The ensemble and configuration of the magnets producing these fields is referred to as the *lattice* of an accelerator. It essentially defines the motion and trajectories of individual particles.

2.1.1. Hill's differential equations

The particle motion in an accelerator is described by a set of periodic differential equations often to referred as Hill's equations [Wil96, p. 58]:

$$\begin{aligned} x''(s) + \left(\frac{1}{R(s)^2} - k(s)\right) x(s) &= \frac{1}{R(s)} \frac{\Delta p}{p} \\ y''(s) + k(s) y(s) &= 0 \end{aligned} \tag{2.1}$$

These describe the horizontal $x(s)$ and vertical displacement $y(s)$ of a particle perpendicular to the reference orbit, as a function of the longitudinal coordinate s along the orbit. The function $R(s)$ denotes the local radius of curvature due to the dipole bending fields. These produce a focussing force in the horizontal plane (weak geometric focussing). The quadrupole strength $k(s)$ describes the strong focussing. It is present in both planes with opposite sign, since a horizontal focussing implies vertical defocussing and vice versa. Net focussing is achieved by using drifts in between the quadrupoles (FODO structure [Hin08, p. 270]). Both $R(s)$ and $k(s)$ are periodic with respect to the orbit length L. The parameter Δp denotes a deviation of the particle's momentum from the nominal momentum p. The effect of the resulting horizontal displacement (dispersion) is described by the inhomogeneous part of the equation.

2.1.2. Betatron oscillations

For an ideal particle with $\Delta p/p = 0$ the differential equations 2.1 simplify and a solution can be given using the Floquet theorem [Hin08, pp. 245–249]:

$$x(s) = \sqrt{\epsilon_x \beta_x(s)} \cdot \cos\left(\Psi_x(s) + \Phi_x\right) \quad ; \quad \Psi_x(s) = \int_0^s \frac{1}{\beta_x(z)}\,\mathrm{d}z \tag{2.2}$$

and $y(s)$ analogously. The particles perform transverse oscillations, the so-called *betatron oscillations*, around the reference orbit. The oscillation amplitude depends on the longitudinal coordinate s and is described by the betatron function $\beta(s)$ and the particle emittance ϵ. The phase is composed of the phase advance $\Psi(s)$ and the particles initial phase Φ. While Φ and ϵ are characteristic to the individual particles and their initial conditions, the betatron function (and thus the phase advance) depends only on the optical properties of the accelerator, given by its magnetic lattice. It can be obtained numerically with standard software for particle accelerator simulation, for example Methodical Accelerator Design (MAD) [Mad].

In transverse phase space, the particle oscillation in x and x' is described by an ellipse [Hin08, pp. 150, 250]. While the particle travels along the orbit, it follows this phase space ellipse (figure 2.1), which itself continuously changes its shape, since it depends on the betatron function and therefore on the longitudinal coordinate s. The ellipse's area $A = \pi\epsilon$ is proportional to the emittance and stays constant while the particle propagates (Liouville's theorem) [Wil96, p. 92].

Particle beam

A beam is an ensemble of typically about 10^8 to 10^{12} particles performing betatron oscillations, each with a certain phase and amplitude depending on the initial con-

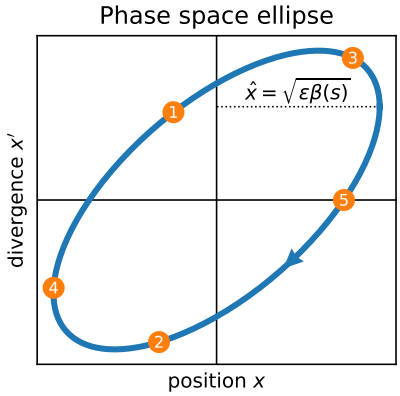

Figure 2.1.: Particle oscillation in the horizontal phase space along the phase space ellipse. The position after each successive turn is indicated by the numbered dots for a fractional tune of $q = 0.6$.

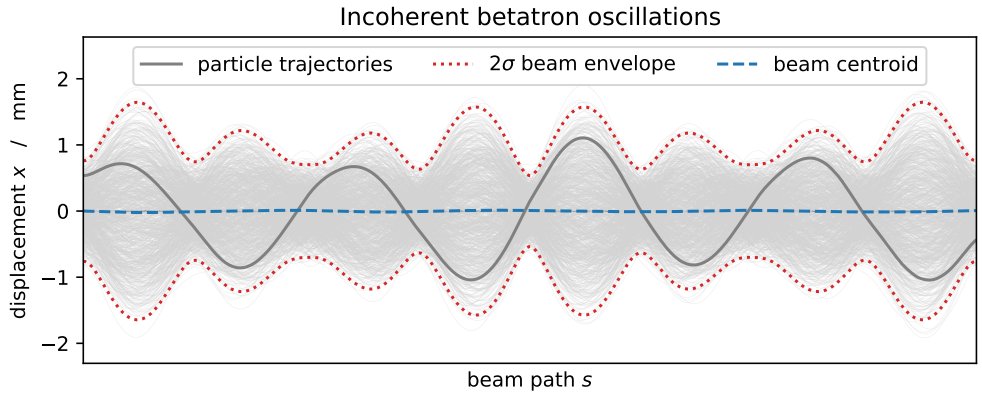

Figure 2.2.: Trajectories of particles performing incoherent betatron oscillations (grey, one particle is emphasized). The centre of charge (beam centroid) is shown in blue and the 2σ beam envelope in red.

ditions. Figure 2.2 visualises a beam consisting of many individual particles. Their betatron oscillations add up incoherently due to the random phase Φ. As a result, the charge centroid of the beam is steady and does not oscillate. This is an important fact when one wants to measure the betatron oscillations (see section 3.2).

The emittance ϵ of the particles usually follows a Gaussian distribution, which is why the beam intensity profile has a Gaussian shape. Its width (beam size) is given by the position dependent beam envelope $E^{1\sigma}(s) = \sqrt{\epsilon^{1\sigma}\beta(s)}$ enclosing 68 % of the particles [Wil96, p. 90]. The parameter $\epsilon^{1\sigma}$ is the (1 sigma) *beam emittance*. Various definitions are used in publications and literature: as an example, figure 2.2 shows the 2 sigma envelope containing 95 % of all particles.

2.1.3. Betatron tune

The betatron tune is defined as the number of betatron oscillations a particle performs during a full turn in the accelerator [Wil96, p. 115]:

$$Q = \frac{f_q}{f_{\mathrm{rev}}} = \frac{\Delta\Psi}{2\pi} = \frac{1}{2\pi}\oint \frac{1}{\beta(s)}\,\mathrm{d}s \tag{2.3}$$

were f_q is the betatron oscillation frequency, f_{rev} is the revolution frequency and $\Delta\Psi = \Psi(L)$ is the phase advance for a full turn. Often only the fractional part of the tune $q = Q - \lfloor Q \rfloor$ is stated.

The particle positions shown in figure 2.1 correspond to a fractional tune of $q = 0.6$, for example $Q = 3.6$. In this example the particle performs 3.6 transverse oscillations each turn and returns to its initial position in phase space after the 5^{th} turn and $5Q = 18$ full betatron oscillations.

Betatron resonances

Imperfections of the magnetic fields are unavoidable and can originate from manufacturing uncertainties, misalignments of magnets or field gradients at the beginning and end of each magnet. Such field errors perturb the particle trajectories. If they occur randomly, the errors average out over many turns and the trajectories remain stable. If, however, the betatron oscillations are resonant with these perturbations, the errors add up coherently leading to an unrestricted increase of the oscillation amplitude. As a result, the beam is lost at the acceptance limit of the accelerator. It is therefore crucial to avoid such resonances during operation of a particle accelerator. [Hin08, pp. 289–306; Wil96, pp. 118–125]

For dipole field errors the resonance condition is fulfilled when the particle passes the imperfection with the same betatron phase each turn (integer tune, $q = 0$). Half integer tune values ($q = 1/2$) result in coherent addition of quadrupole field errors every second turn. Higher order field errors lead to resonances at multiples of $1/n$ respectively. While these resonances exist independently in the horizontal and vertical plane, there are also coupled resonances. These originate from field errors affecting both planes, e.g. tilted magnets or the coupling terms of higher order multipoles. In general, the condition for resonances of the order $|m| + |n|$ reads:

$$mQ_x + nQ_y = p \qquad ; \quad m, n, p \in \mathbb{Z} \tag{2.4}$$

Figure 2.3 shows the tune diagram with resonance lines up to the 4^{th} order. While the number of resonances increases with the order, their strength (width) decreases. Typically, resonances up to the 5^{th} order have to be taken into account when choosing an appropriate working point for an accelerator in a region free of resonance lines. [Wil96, p. 125]

2.1.4. Dispersion

In the previous sections it was assumed that all particles have equal momentum. However, a real beam consists of particles whose momenta are distributed around the nominal momentum p. For a particle with a momentum deviation $\Delta p \neq 0$ the bending radius $R \propto p$ of the trajectory inside the dipole magnets differs. As a result, the particle trajectory is shifted towards the out- or inside of the accelerator:

$$x_p(s) = x(s) + \underbrace{D(s)\frac{\Delta p}{p}}_{x_D(s)} \tag{2.5}$$

where $x(s)$ are the horizontal betatron oscillations (equation 2.2) and $x_D(s)$ is the dispersive orbit shift described by the *dispersion* $D(s)$ [Hin08, pp. 263 sq.]. As a result, the respective orbit length is in- or decreased.

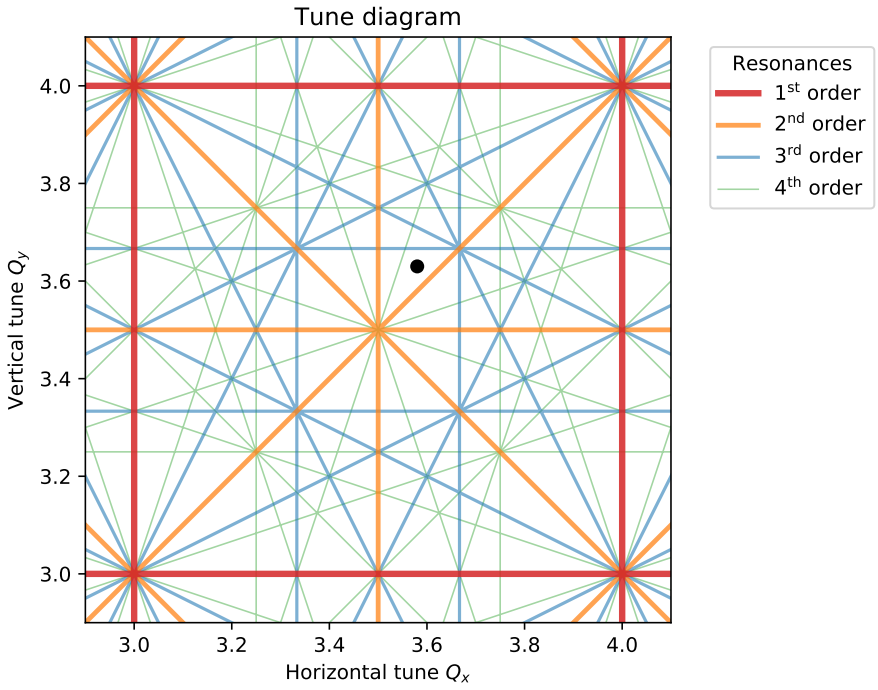

Figure 2.3.: Tune diagram with resonance lines up to the 4$^{\text{th}}$ order. The working point is marked with a black dot.

2.1.5. Chromaticity

Similar to the dipole bending radius, also the focussing strength of a quadrupole magnet $k \propto p^{-1}$ depends on the particle's momentum. In linear approximation, a momentum deviation therefore results in a focussing error of $\Delta k \propto -\Delta p/p$.

Both, quadrupole focussing and radius of curvature, essentially define the equations of motion 2.1 and their solutions. Therefore, a momentum deviation directly leads to a tune shift ΔQ. This effect is called *chromaticity*. The natural[1] chromaticity is defined as:

$$\xi_{\text{nat}} = \frac{\Delta Q}{\Delta p/p} = \frac{1}{4\pi} \oint k(s)\beta(s)\,\mathrm{d}s \tag{2.6}$$

In certain literature[2] the relative chromaticity ξ/Q is used in place of ξ. The natural chromaticity is always negative because stable beam operation requires net focussing, which means that the full-turn-integral $\oint k(s)\,\mathrm{d}s$ must be negative. [Wil96, pp. 135 sqq.; Hin08, pp. 297 sqq.; Wie15, pp. 509 sqq.]

[1] The term *natural* indicates that the effect of sextupole magnets is not included

[2] While the above definition is common for beam optics textbooks, many measurement related papers use ξ to denote the *relative* chromaticity. All equations in this thesis — even if originally taken from such literature — were modified to match the definition as per equation 2.6.

Tune spread

In an accelerator the beam momentum is typically Gaussian distributed. This momentum spread leads to an intrinsic width of the tune (*tune spread*) by the effect of chromaticity. For large chromaticities the tune spread can become so large that the resonances described in section 2.1.3 can not easily be avoided. For stable operation of an accelerator, it may therefore be important to compensate the chromaticity.
The tune is additionally broadened by other mechanisms, mainly non-linear fields and collective effects, such as intra-beam scattering or space charge [Wie15, pp. 543, 723].

Chromaticity compensation with sextupoles

A large natural chromaticity can be compensated using sextupole magnets. While the magnetic field strength of a quadrupole linearly increases with an offset from its centre, the field of a sextupole is proportional to the square of the offset. This means that a sextupole's focussing strength – which is proportional to the field gradient – increases linearly with the horizontal[3] offset: $k_{\text{sex}} = mx$.

In order to compensate the quadrupole focussing error $\Delta k \propto -\Delta p/p$, the sextupoles are placed in regions with large dispersion D. In the dispersive sections the momentum deviation Δp leads to a horizontal offset $x_D = D\Delta p/p$. This subsequently leads to a momentum dependent focussing in the sextupoles: $k_{\text{sex}} \propto \Delta p/p$. With a proper choice of the sextupole strength m the focussing error of the quadrupole magnets can thereby be compensated to achieve a small value for the chromaticity.
A single group of sextupole magnets affects the horizontal and vertical plane equally. To compensate the chromaticity independently in both planes, at least two groups of sextupoles have to be arranged at places with different betatron function in the respective plane. [Wie15, pp. 513 sq.; Hin08, pp. 299 sq.]

Taking the effect of sextupoles into account, the *total* chromaticity is:

$$\xi = \frac{\Delta Q}{\Delta p/p} = \frac{1}{4\pi} \oint \big[k(s) + m(s)D(s)\big]\beta(s)\,\mathrm{d}s \tag{2.7}$$

[3] Rotating the magnet by 30° would make the *vertical* offset determining (which is undesirable)

2.2. Longitudinal linear beam dynamics

In circular accelerators, cavities are used to control the energy of the particle beam. Inside the cavity the force of a radio frequency (RF) alternating field accelerates or decelerates the particles. Since stable, phase-focused acceleration is only possible during a half-period of the alternating field, the particle beam has to be bunched. Just like the betatron oscillations in transverse phase space caused by quadrupole focusing (see section 2.1.2), the particles also oscillate in longitudinal phase space due to phase-focusing. During these *synchrotron oscillations* the particle oscillates back and forth inside the bunch, periodically gaining and losing small fractions of its energy. [Wil96, pp. 201 sqq.]

Revolution frequency and momentum

The revolution frequency $f_{\mathrm{rev}} = v/L$ of a circulating bunch depends on its velocity v and the length L of the closed orbit, which is influenced by the rigidity of the dipole magnets. In linear approximation the latter dependence is expressed by the *momentum compaction factor*:

$$\alpha_{\mathrm{p}} = \frac{1}{\gamma_{\mathrm{tr}}^2} = \frac{\Delta L/L}{\Delta p/p} = \frac{1}{L} \oint \frac{D(s)}{R(s)} \, \mathrm{d}s \tag{2.8}$$

with the *transition energy* γ_{tr} as a characteristic property. The relation between a change in revolution frequency Δf_{rev} and a change in momentum Δp is then described in linear approximation by [Wie15, p. 249]:

$$\frac{\Delta f_{\mathrm{rev}}}{f_{\mathrm{rev}}} = \frac{\Delta v}{v} - \frac{\Delta L}{L} = \left(\frac{1}{\gamma^2} - \alpha_{\mathrm{p}} \right) \frac{\Delta p}{p} = \eta \frac{\Delta p}{p} \tag{2.9}$$

The proportionality factor is the *slip factor* $\eta = \gamma^{-2} - \alpha_{\mathrm{p}}$. Depending on whether the change in velocity or the change in orbit length dominates, this factor can be either positive or negative. For energies below the transition energy ($\gamma < \gamma_{\mathrm{tr}}$) the slip factor is positive and the frequency increases with the beam momentum. For $\gamma > \gamma_{\mathrm{tr}}$ the dependence is reversed ($\eta < 0$). At the transition energy the slip factor vanishes and phase focusing becomes impossible. [Hin08, pp. 267 sq.]

3. Beam Diagnostics

3.1. Beam position monitors

A beam position monitor (BPM) is a device used to determine the horizontal and vertical position of the particle beam inside an accelerator. It most commonly comprises capacitive pick-up electrodes sensitive to the beam position and associated readout electronics.

Capacitive pick-up

A capacitive pick-up exploits the fact, that any charge induces an image charge on a nearby conducting surface. Two electrodes are placed inside the vacuum chamber on opposite sides of the beam to pick up the image signal of a passing bunch of charged particles. The charge induced on the electrodes is proportional to the charge of the bunch and dependent on its distance to the respective electrode. While the bunch passes, it produces a measurable displacement current flowing onto the electrodes as it approaches and then off again as it leaves.
The transverse bunch position can be reconstructed from the difference between the integrated signal of the left (I_L) and the right electrode (I_R). To cancel out the dependence on the total charge, one normalizes the signals (difference over sum):

$$\frac{\Delta}{\sum} = \frac{I_\mathrm{R} - I_\mathrm{L}}{I_\mathrm{R} + I_\mathrm{L}} = \zeta x + \text{non-linear terms}$$

In first order approximation this ratio is proportional to the transverse beam position where ζ is the sensitivity. In general there are additional non-linear and coupling terms which depend on the pick-up's geometry and have to be compensated for.
Button like electrodes are one of the most simple geometries available but have the disadvantage of a high non-linearity and low sensitivity. By using longer electrodes, the sensitivity can be increased (strip-line design). Yet a good linearity can only be achieved with the *split-plane* geometry, consisting of a cylinder barrel that is diagonally cut into two electrodes. [Sha92; Wen18]

At COSY the split-plane BPM type is used, with an inner diameter of 150 mm and a length of 100 mm [Mai90]. In total 29 BPMs are placed around the ring, each consisting of two electrode pairs for the horizontal and vertical plane respectively.

3.2. Tune measurement

To measure the betatron tune, the betatron oscillation frequency has to determined with respect to the revolution frequency. Therefore, a pick-up structure sensitive to the transverse beam position is used. Since the oscillation amplitude is usually too small to get a sufficient signal, the betatron oscillations are resonantly excited. The fluctuations of the pick-up signal then allow to reconstruct the transverse oscillations. Their frequency is determined after a Fourier transform of the time structure into frequency space. [Jon18; Ste09]

3.2.1. Excitation of betatron oscillations

As shown in section 2.1.2 and figure 2.2, the particle oscillations inside a beam are incoherent and the remnant coherent fraction is tiny. The oscillation of the beam centroid is typically in the sub-micrometer range [Jon18, p. 244], which is below the sensitivity of most detector systems. External excitation is required to achieve a sufficient signal-to-noise ratio when measuring the betatron oscillation amplitude using a beam position sensitive device.
The excitation enforces a common phase on the particles such that their individual oscillations become coherent as depicted in figure 3.1. As a result, the beam centroid starts to oscillate and these oscillations can be measured.

The beam can either be excited by applying a single kick or an RF signal to the beam. In the latter case the excitation frequency f_{ex} has to be resonant with the beam oscillation: $f_{\mathrm{ex}} = (n \pm q) f_{\mathrm{rev}}$, $n \in \mathbb{Z}$. Since the tune q is not known a priori, one can either vary the frequency by sweeping it across the range where the tune is expected, or use a signal composed of frequencies in the expected range (band limited white noise). The RF excitation has the advantage, that by choosing an appropriate

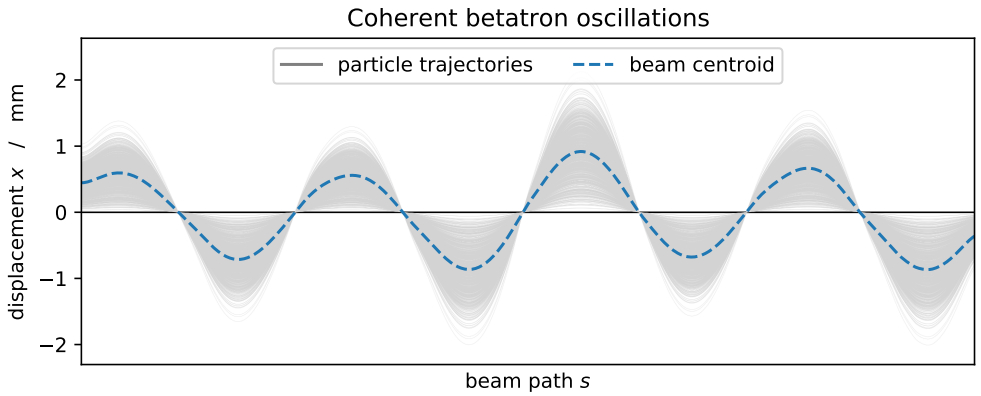

Figure 3.1.: Trajectories of particles performing coherent betatron oscillations. As a result, the beam centroid also oscillates.

bandwidth, the spectral power density can be increased and excitation of other unwanted resonances can be avoided [Ste09, p. 330].

After the excitation is switched off, the individual oscillations start to diverge due to the differences in their momenta until they become incoherent again. Therefore, the measurement is only possible while the excitation is active and during the typically short decoherence time afterwards.

3.2.2. Pick-up signal and its Fourier transform

Each time a bunch of particles passes the pick-up structure, a short signal pulse proportional to the transverse position is measured. The delta signal of the pick-up shows a train of pulses evenly spaced in time by the revolution period $T_{\mathrm{rev}} = 1/f_{\mathrm{rev}}$ as depicted by the continuous signal in figure 3.2a. Since the transverse position oscillates around the (non-zero) beam position, the pulse height is modulated with the (fractional) betatron frequency $f_q = q f_{\mathrm{rev}}$.

As derived in appendix A.1, the Fourier transform of this continuous signal leads to the frequency spectrum shown in figure 3.2b. The peaks at the revolution harmonics $h f_{\mathrm{rev}}$ are accompanied by betatron sidebands located at $f_\pm = h f_{\mathrm{rev}} \pm f_q$ which originate from the modulation of the pulse height. The distance of these sidebands to the corresponding harmonics — normalized to the revolution frequency — corresponds to the fractional tune: [Cas09, pp. 415 sqq.]

$$q = \frac{f_q}{f_{\mathrm{rev}}} = \frac{f_+ - f_-}{2 f_{\mathrm{rev}}} \tag{3.1}$$

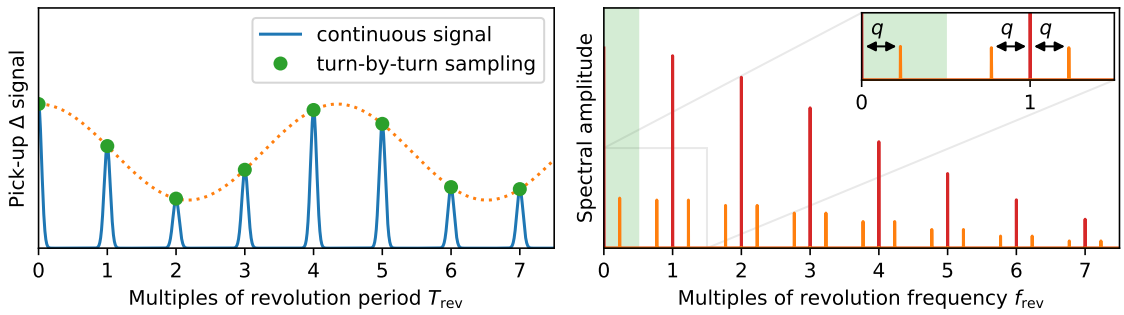

(a) Signal in time domain with the pulse height being modulated by the betatron oscillation.

(b) Signal in frequency domain with revolution harmonics (red) and betatron sidebands (orange).

Figure 3.2.: Difference signal at a pick-up for an off-centre bunched beam performing betatron oscillations. While a continuous signal in time leads to a unbounded frequency spectrum, discrete turn-by-turn sampling reduces the observable frequency range to the region shaded in green.

Instead of the continuous pick-up signal, it is also possible to use the time discretised beam positions from a BPM. Here, only one position value is obtained each turn (turn-by-turn sampling). The Nyquist-Shannon theorem states that for a signal sampled at a frequency f_s, only frequencies $f < f_s/2$ can be reconstructed. For the case of turn-by-turn sampling this reduces the observable frequency range to the first half of the revolution frequency, as indicated by the shaded region in figure 3.2b. In this limited region, only a single betatron sideband appears. To determine the tune, one has to decide whether the observed sideband is the upper sideband at $f_+ = qf_{rev}$ or the lower sideband of the first harmonic at $f_- = (1-q)f_{rev}$. In general q and $1-q$ can not be distinguished from a single measurement. The ambiguity can be resolved by varying the tune in a controlled manner and observing in which direction the betatron sideband moves [Jon18, p. 242]. However, usually this is not required since the approximate range of the tune is known from model calculations.

3.2.3. Different measurement methods

Implementations of tune measurements vary by the type of excitation, the hard- and software used and the way the tune is determined from the frequency or phase information. In the following an overview is given on the various methods.

Schottky monitor

Schottky diagnostics trace back to the physicist Walter Schottky, who first described the concept of current fluctuations (shot noise) in 1918. A Schottky monitor exploits this concept by detecting the current fluctuations of a particle beam with a pick-up structure. Using a spectrum analyser, these fluctuations are observed as distinct bands in the frequency spectrum. Since the longitudinal spectrum obtained from the sum signal of a pick-up is dominated by the momentum fluctuations, it can be used to gain information on the momentum distribution and synchrotron motion. Fluctuations of the transverse beam position are contained in the delta signal (see section 3.1). The corresponding transverse spectrum therefore provides information on the transverse momentum distribution and betatron motion. [Bet17]

When the betatron oscillations are excited with broadband noise, a Schottky monitor connected to the delta signal of a suitable pick-up can be used to observe the betatron sidebands at $f_\pm$. For unbunched (continuous) beams the revolution harmonics are absent, but for bunched beams with a sufficient transverse offset they can still be observed. If the spectrum analyser is configured to display the frequency spectrum around the h^{th} harmonic, the tune is given by [Cas09, p. 416]:

$$q = \frac{f_+ - f_-}{2f_{rev}} = h\frac{f_+ - f_-}{f_+ + f_-} \tag{3.2}$$

The advantage of a Schottky monitor is its applicability to bunched as well as continuous beams. Depending on the sensitivity of the pick-up used, the excitation can be

relatively low. However, to get a reasonable good resolution the acquisition time has to be in the order of a second, which is relatively slow compared to other methods. Besides the tune, a Schottky monitor can also be used to determine a variety of other parameters — revolution frequency, beam momentum, momentum spread, synchrotron tune or chromaticity — which makes it a multi-purpose diagnostic tool. [Cas09]

Regular beam position monitor

With sufficient excitation, a standard BPM can be used to detect the oscillation of the beam centroid. The position is determined each time the particle bunch passes by (turn-by-turn sampling). The sampled beam positions undergo a discrete Fourier transform (DFT) yielding the frequency spectrum. The tune is finally extracted from the sideband in the normalized frequency spectrum as described in section 3.2.2.

For efficient computation of the DFT, fast Fourier transform (FFT) algorithms exist, which iteratively decompose the calculations into smaller parts. For a signal of N samples, "the FFTs considerably reduce the computational cost for computing the DFT(N) from $2N^2$ to $\mathcal{O}(N \log N)$ arithmetic operations" [Plo18, p. 231]. A particularly well known algorithm is the radix-2 FFT by Cooley and Tukey [Coo65] where the calculations are iteratively split into half. To make use of this algorithm, the number of sampled beam positions must be a power of two ($N = 2^n$).

Since BPMs exist in any accelerator, this method does not require additional hardware and is therefore cost saving. However, it is only applicable to bunched beams and typically requires large excitation power, since the dynamic range of a BPM is usually small. [Jon18, p. 244]

Base-band tune system

To overcome the dynamic range limit of a regular BPM, a dedicated analogue signal processing is needed, sensitive only to changes of the beam position, but indifferent regarding the absolute beam position. Such a system is the base-band tune (BBQ) system [Gas05], which is able to resolve sub-micrometer betatron oscillations. Since remnant beam oscillations of this magnitude are typically present, only a very weak or even no excitation at all is required for the measurement. [Jon18, pp. 244 sq.] While such a system allows for non-invasive and therefore continuous monitoring of the tune, it is typically less precise than methods relying on a strong excitation due to the relatively large noise level.

Beam transfer function measurement

In a beam transfer function (BTF) measurement the beam is excited with a sinusoidal signal of precisely known frequency and phase. The frequency is swept over the range of interest, while the amplitude and phase of the betatron oscillations are recorded as

a function of the frequency, e.g. by means of a network analyser [Bou95, p. 775]. The tune resonance can not only be derived from the peak in the amplitude spectrum, but also from the point of maximum slope in the phase response at $\varphi = \pi/2$.
Sweeping the excitation frequency allows for a precise determination of the phase and therefore increases the measurement accuracy. However, it also requires more time and makes this measurement method slow. The time resolution can be improved by sweeping the frequency rapidly (chirp excitation) on the cost of a less precise measurement [Sch97, pp. 43 sq.].

Phase-locked loop tune tracker

A phase-locked loop (PLL) tune tracker continuously adjusts the excitation frequency to match the betatron tune [Tan06, pp. 615 sqq.]. The control variable of such a closed-loop system is the phase of the beam oscillation, which is regulated to match the resonance condition $\varphi = \pi/2$. Such a system allows to track the time evolution of the tune very precisely with a resolution in the order of 10^{-6} [Ste09, p. 341]. Yet it requires a sophisticated regulation circuit so as not to get locked at parasitic resonances.

3.3. Chromaticity measurement

Classically, chromaticity is measured by slightly varying the beam momentum and measuring the corresponding tune change with either of the methods described in section 3.2. Since changing the momentum and tune affects beam operation, this approach might not always be feasible and alternative methods can be preferable.
Most of the methods described in this section require knowledge of the slip factor η. It can be obtained from model calculations [Mad] or by measuring the momentum compaction factor.

3.3.1. Momentum change based methods

The momentum of a particle beam can be changed by adjusting either the RF frequency or the magnetic bending field of the dipoles:

RF frequency change

A small change of the RF frequency results in a momentum change proportional to the inverse slip factor η^{-1} as described in section 2.2. The chromaticity can then be determined by measuring the subsequent tune change: [Wil96, p. 339; Jon18, p. 248]

$$\xi = \frac{\Delta Q}{\Delta p/p} = \eta \frac{\Delta Q}{\Delta f/f} \tag{3.3}$$

Since the magnetic bending fields are kept constant during the measurement, the change in momentum also makes the beam go on an outer (or inner) orbit. The resulting change in the horizontal beam position causes the sextupole fields to contribute to the tune change as described in section 2.1.5. The measured value is consequently the *total* chromaticity.

Dipole bending field change

An alternative method to change the momentum is to adjust the magnetic bending field while keeping the RF frequency constant. The subsequent momentum change is given by (see appendix A.2):

$$\frac{\Delta p}{p} = \frac{1}{1 - \gamma_{\mathrm{tr}}^2/\gamma^2} \frac{\Delta B}{B} \approx \frac{\Delta B}{B} \tag{3.4}$$

The latter approximation is valid for energies well above transition ($\gamma \gg \gamma_{\mathrm{tr}}$). In this limit the change in bending radius $R = p/(qB)$ is negligible since $\Delta R/R = \Delta p/p - \Delta B/B \approx 0$ and hence the orbit is kept constant. This means that — in contrast to the previously described method — sextupole and higher order fields do not contribute to the observed tune change. Thus this method allows to measure the *natural* chromaticity instead [Ste09, p. 347]. It is again obtained from the measured tune change:

$$\xi_{\mathrm{nat}} = \frac{\Delta Q}{\Delta p/p} \approx \frac{\Delta Q}{\Delta B/B} \tag{3.5}$$

3.3.2. Passive methods

The methods described in this section do not interfere with beam operation since no active change of the beam momentum and tune is required.

Schottky monitor: width of betatron sidebands

The transverse Schottky spectrum does not only allow to determine the tune (section 3.2.3), but also provides a non-invasive method to measure the chromaticity. The width $\Delta f_{\pm}$ of the betatron sidebands at the h^{th} harmonic is primarily determined by the momentum spread $\Delta p/p$, but also depends on the fractional tune q and the chromaticity [Bou95, p. 753]:

$$\Delta f_{\pm} = f_{\mathrm{rev}} \frac{\Delta p}{p} \left[(h \pm q)\, \eta \pm \xi \right] \tag{3.6}$$

The dependence on the chromaticity is of opposite sign for the upper and lower sideband respectively. While the power (area) in both sidebands is equal, the width Δf_+ of the upper sideband is slightly larger than the width Δf_- of the lower sideband

(see figure 3.3). The chromaticity can be reconstructed from the measured widths in the Schottky spectrum as [Cas07, p. 46]:

$$\xi = \eta \left(h \frac{\Delta f_+ - \Delta f_-}{\Delta f_+ + \Delta f_-} - q \right) \tag{3.7}$$

While the resolution of this method is limited by the noise in the Schottky signals, its sensitivity is best for unbunched beams observed at low harmonics [Jon18, p. 250]. Since no change of the beam momentum is required, the measurement does not interfere with beam operation and can be used for passive monitoring.

Schottky monitor: amplitude of synchrotron sidebands

For bunched beams, synchrotron sidebands can be observed in the Schottky spectrum. The synchrotron motion in longitudinal phase space modulates the particle's momentum. Since the chromaticity couples this momentum change to the transverse betatron motion, the tune is modulated and additional synchrotron sidebands appear on either side of the betatron sidebands as shown in figure 3.3. Their amplitude scales with the chromaticity, but is effected by a number of additional factors like bunch length and synchrotron frequency. These effects have to be quantified empirically before the chromaticity can be determined from a measurement [Reh10, p. 45].
Since this measurement method relies on the synchrotron motion, it is only applicable to bunched beams with a sufficient synchrotron tune such that the sidebands are clearly distinguishable from the tune resonance. Moreover, only the magnitude but not the sign of the chromaticity can be determined.

Head-tail phase shift

While a particle performs synchrotron oscillations, its longitudinal position inside the bunch and its momentum constantly change. The momentum reaches a maximum at

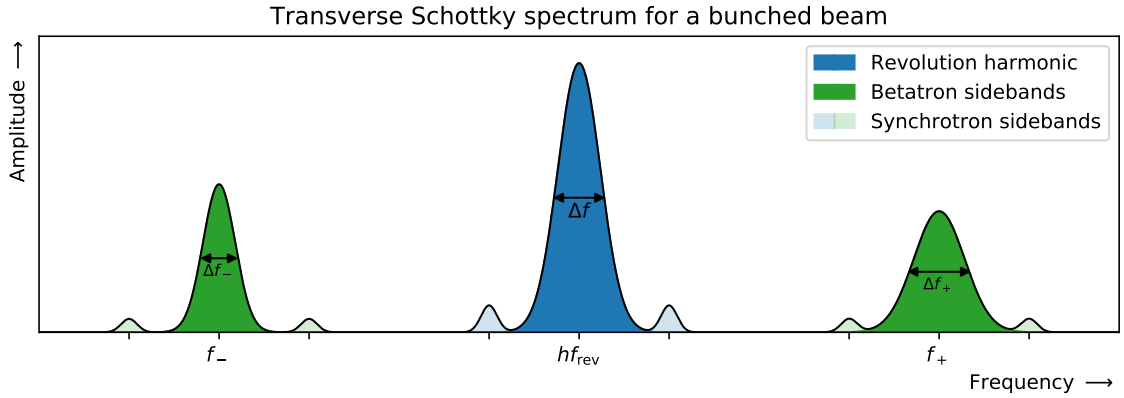

Figure 3.3.: Transverse Schottky spectrum (schematic) with revolution harmonic, betatron sidebands at $f_\pm = (h \pm q) f_{\mathrm{rev}}$ and respective synchrotron sidebands.

the head of the bunch and a minimum at its tail respectively. Since the chromaticity couples this momentum difference to the betatron motion, the phase of the betatron oscillation differs between head and tail of a single bunch. This is referred to as *head-tail phase shift* [Coc98]. Depending on the sign and magnitude of the chromaticity, this phase difference can lead to labile beam motion (head-tail-instabilities [San69]), because the bunch's tail is influenced by the wake field of its head.
Although being an undesirable effect, the phase difference can be used to measure the chromaticity. Therefore, the transverse position of the head and tail of a bunch has to be monitored separately over the course of a synchrotron period. After the phase has been reconstructed, the phase difference $\Delta\varphi$ is calculated, which reaches a maximum after half a synchrotron period. This maximum phase difference $\Delta\varphi_{\max}$ is proportional to the chromaticity ($\Delta\tau$ denotes the bunch length): [Coc98, p. 284]

$$\xi = \eta \frac{\Delta\varphi_{\max}}{4\pi f_{\mathrm{rev}} \Delta\tau} \tag{3.8}$$

This method has been demonstrated [Coc98], but is not routinely used since it is difficult to determine the position of the head and tail separately. Additionally, the phase measurement requires a sufficient bunch length and coherence during a full synchrotron period [Jon18, p. 253].

4. Development of a Fast Tune Measurement System

4.1. Measurement principle

The developed tune measurement system exploits the capabilities of the existing BPMs at COSY to determine the tune as described in section 3.2.3. The signal of each capacitive pick-up is amplified by dedicated preamplifiers and subsequently processed by the Libera Hadron beam position processor [Žni16; Kam19]. This device digitizes the signal with a 16 bit analog-to-digital converter (ADC) at 250 MHz. A dedicated algorithm is used to detect individual bunches and to calculate the bunch position (see section 3.1). The instrument finally provides the horizontal and vertical beam position together with a timestamp for every bunch (bunch-by-bunch data).
To be able to measure the tune, betatron oscillations are excited by applying a band limited white noise signal via a stripline kicker. Afterwards, a small amount of the bunch-by-bunch position data corresponding to the excited transverse oscillations is read out and analysed. The tune is extracted from the data by performing a DFT and fitting the resulting tune peak in the frequency spectrum.

COSY is equipped with 29 BPMs distributed around the ring. The sensitivity of the tune measurement can be increased by choosing a BPM at a location where the betatron function – and thus the betatron oscillation amplitude – is large. Therefore, all the available BPMs can be selected for the tune measurement. This approach also allows flexibility in case of malfunctions of some BPMs and provides a means to cross-validate the measurement with different, independent diagnostic devices.

In the following sections the various aspects of excitation, data analysis and integration of the tune measurement into the COSY control system are discussed.

4.2. Noise excitation

The betatron oscillations are excited using band limited white noise. Its spectral power density can be adjusted by choosing an appropriate frequency range and signal voltage. This excitation method has the benefit of being fast and thus causing the least beam loss. Therefore, the requirements of a short measurement time and multiple measurements per cycle can be fulfilled.

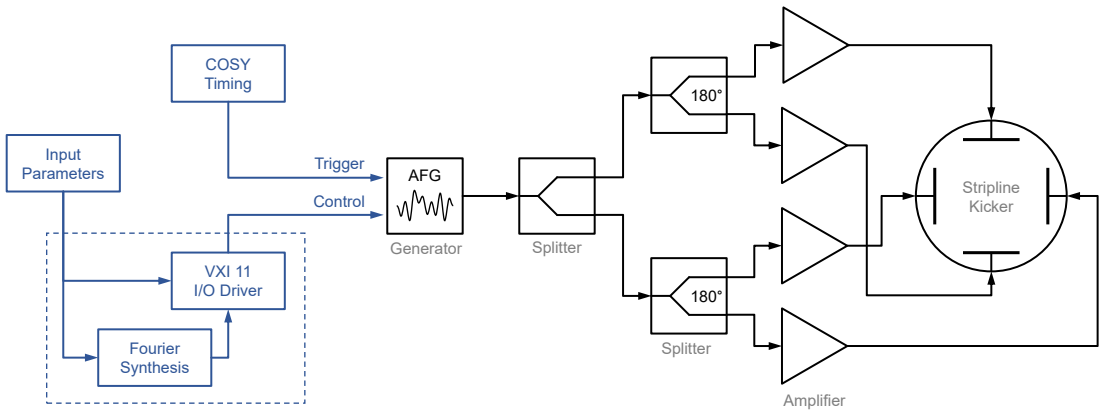

Figure 4.1.: Signal-flow graph of the noise excitation system with controller software (blue) and RF hardware components (black)

Figure 4.1 shows the signal-flow graph of the noise excitation system. An arbitrary function generator (AFG) is used to generate the excitation signal from a noise sequence stored in its memory. The generator, a Tektronix AFG3021C with an output frequency of up to 25 MHz, is controlled by a Python program over Ethernet using the VXI-11 protocol. Besides setting general parameters like voltage level, signal duration and delay, the implementation also takes care of computing the noise sequence and uploading it to the device as a custom waveform. Given the frequency band, sampling frequency and sample length, the noise sequence is computed via an inverse Fourier transformation (Fourier synthesis) with random phase. The voltage level is then scaled according to the desired average power of the generated signal.

The AFG is triggered via the COSY timing system. Optionally, an automatic software trigger linked to the existing BPM trigger can be used to simplify the configuration procedure, especially if many measurements are envisaged within a machine cycle. On the trigger signal, the AFG outputs the noise sequence in burst mode for the specified duration.

The output signal from the generator is divided using a two-way splitter for the horizontal and vertical plane and two subsequent 180° splitters inverting the signal polarity. Each of the four channels is then amplified separately with a power amplifier, before the RF signal is guided to the 1.05 m long electrodes of the stripline kicker. The connection is made such, that the signals applied to opposite electrodes are of opposite polarity in order to produce a transverse electric field.
During initial tests it became apparent that the existing 15 W power amplifiers of the stripline kicker were not sufficient for tune measurements at high beam momenta above 1 GeV/c, since the excitation of betatron oscillations was too weak. Therefore, the system was connected to the 150 W power amplifiers of the currently unused transverse damping system to increase the excitation power.

4.3. Data analysis

Shortly after the excitation, the acquired bunch-by-bunch position data is read out from the Libera Hadron processors and subsequently analysed to determine the tune. Optionally, an additional background measurement prior to the excitation can be performed. By subtracting the background spectrum, spurious signals can be eliminated from the frequency spectra and the signal-to-noise ratio is improved, allowing for a more precise tune measurement.
With sufficiently long excitation a continuous tune measurement over several seconds can be performed. This allows to investigate the tune evolution over time, e.g. during the acceleration ramp.

4.3.1. Readout of bunch-by-bunch data

The readout of the bunch-by-bunch data is automatically started with a sufficient delay after the data acquisition of the Libera Hadron processors was triggered by the COSY timing system. The positions as well as the timestamps of the detected bunches are transferred via the Channel Access (CA) protocol. This protocol is a standard of the Experimental Physics and Industrial Control System (EPICS), which is the control system being used at COSY. Since the amount of data to be transferred can become considerably large for continuous tune measurements over several seconds, the download needs to be performed in chunks. Thereby the integrity of the data has to be ensured, especially for cases where some bunches were not detected correctly, e.g. due to low beam intensity. This is achieved by special handling of duplicate or missing timestamps, heuristic checks for leftover data in the Libera Hadron's buffers as well as plausibility verifications on frequency, bunch number and position values.

The bunch timestamps are used to select a subsample in the data corresponding to the excited betatron oscillations. If the optional background measurement is enabled, an additional subsample prior to the excitation is also extracted for analysis. Moreover, the revolution frequency is calculated from these timestamps.

The resolution of the tune measurement is directly determined by the length of the subsample used for the spectral analysis. For a signal consisting of N bunch positions sampled at the revolution frequency, the discrete frequency spectrum is limited by the Nyquist frequency at $f_{\mathrm{rev}}/2$. Therefore, the spectrum consists of $N/2$ points in the range of $r = f/f_{\mathrm{rev}} \in [0, 0.5]$, limiting the resolution to $1/N$.
To achieve a precision of 10^{-3} (three digits), bunch positions for at least 1000 consecutive turns have to be acquired. The number of turns has to be multiplied with the number of stored bunches per turn given by the harmonic h of the COSY RF. Rounding up to the next power of two allows to use the fast radix-2 FFT algorithm for numerical computation of the DFT (see section 3.2.3). The default subsample size used for the analysis was chosen as $N = 2^{13} = 8192$ bunches, but can be configured at runtime. This ensures a high resolution even for $h = 4$ while keeping the required

measurement time and computational costs low. Considering a revolution frequency from 0.5 MHz to 1.6 MHz and $1 \leq h \leq 4$ for COSY, the required measurement time ranges from 2.5 ms to 33 ms.

4.3.2. Fourier transform and tune resonance fit

A discrete Fourier transform (DFT) is performed on the bunch position subsamples by means of an FFT algorithm implemented using the NumPy library [Num; Coo65]. This process is repeated for both, the horizontal and vertical plane, as well as the optional background measurement. After subtraction of the background, the spectra are smoothened by a moving average filter to reduce the residual noise and filter out spikes. As a result, the frequency spectrum normalized to the bunch frequency is obtained. Multiplication with the number of stored bunches h yields the resonance spectrum in units of $r = f/f_{\mathrm{rev}}$. The spectrum is cropped to the first half interval from 0 to 0.5 since the $h - 1$ repeated mirror images above $r = 0.5$ contain no additional information.

Figure 4.2 shows the obtained frequency spectra for an exemplary tune measurement. The non-vanishing width of the betatron resonance peak is the result of the mechanisms described in section 2.1.5. Since it is the superimposed signal of many independent particles, the peak can adequately be described by a normal Gaussian distribution according to the central limit theorem. The chromaticity induced tune broadening is typically also of Gaussian shape since the beam momentum is usually normal distributed.
Using a least square optimisation, a Gaussian distribution is fitted to each of the obtained spectra as shown by the close-ups in figure 4.2. This yields the fraction $\hat{r}$ as the mean of the distribution, from which the tune can be deduced as $q = \hat{r}$ or $q = 1 - \hat{r}$ (see section 3.2.2). The distinction is made based on the *tune search range*, which can be adjusted by the operator. This range is also used to limit the fit to a certain region of the spectra and to calculate the absolute tune from the fractional one. The default

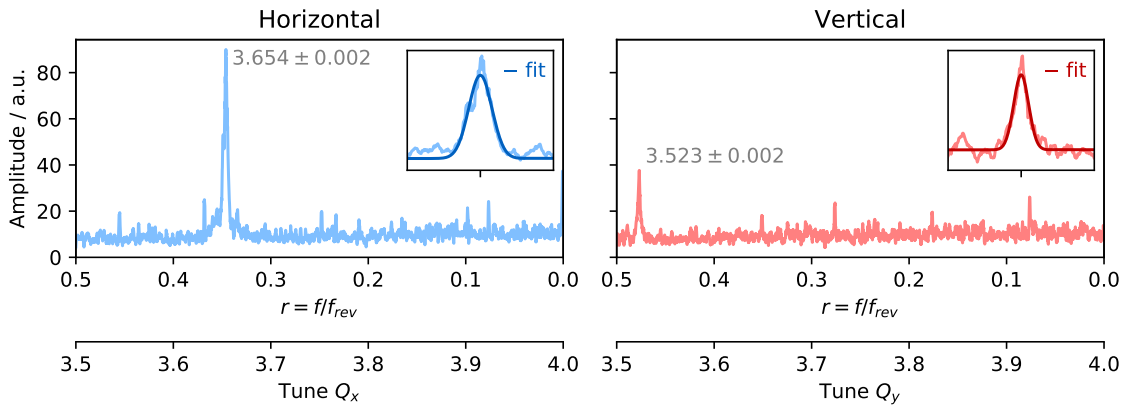

Figure 4.2.: Frequency spectra of a tune measurement with Gaussian fits (close-ups)

tune search range for the lattice of COSY is $Q \in [3.5, 3.7]$ corresponding to a fitting range of $r \in [0.3, 0.5]$ and an absolute tune of $Q = 4 - \hat{r}$. The fit is only accepted if the fitted tune peak is significantly outside the noise level, that is, if the peak amplitude is larger than six standard deviations of the background signal. The measurement uncertainty is computed by summation in quadrature of the fit uncertainties and the intrinsic tune width (standard deviation of the Gaussian). In the following this uncertainty is denoted with a "±" to emphasize that it also includes the tune spread. The procedure is repeated separately for both planes yielding the horizontal tune Q_x and the vertical tune Q_y with respective uncertainties. Finally, the values and uncertainties of all successful measurements across multiple BPMs are combined.

For cases where the transverse motion is coupled[1], the spectra can contain two resonance peaks with different intensities each (figure 4.3). To distinguish the two tunes Q_1 and Q_2 the search range can be adjusted accordingly. An option to determine both tunes from a single measured plane is also implemented. One has to note, however, that for strong coupling and $Q_x \approx Q_y$, the two measured tunes Q_1 and Q_2 do not correspond to the vertical and horizontal tune but will stay separated. [Wie15, pp. 692 sqq.]

4.3.3. Continuous tune measurement

The tune can also be monitored continuously for several seconds by exciting the betatron oscillations during the complete timeframe of interest. This way the tune can be tracked e.g. during the acceleration ramp.
For the continuous tune measurement, bunch-by-bunch positions with $N = \mathcal{O}(10^6)$ samples are loaded from the Libera Hadron for a single BPM of choice. The time dependent frequency spectra (spectrograms, figure 4.4) are calculated via a short-time

[1] Coupling can occur due to rotated magnetic fields or in presence of longitudinal fields. The latter are generated by solenoids as used for electron cooling — a routine operation at COSY.

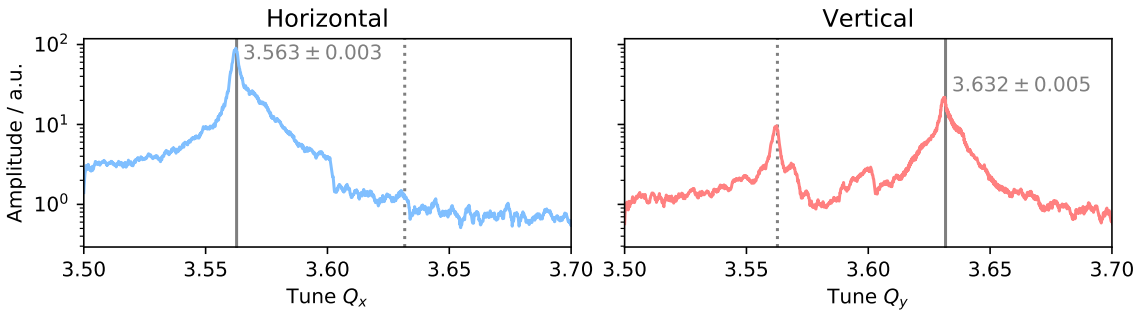

Figure 4.3.: Frequency spectra of a tune measurement with coupling (logarithmic scaling). The horizontal tune at $Q_x = 3.563 \pm 0.003$ couples to the vertical plane and appears as a second smaller peak in the vertical spectrum.

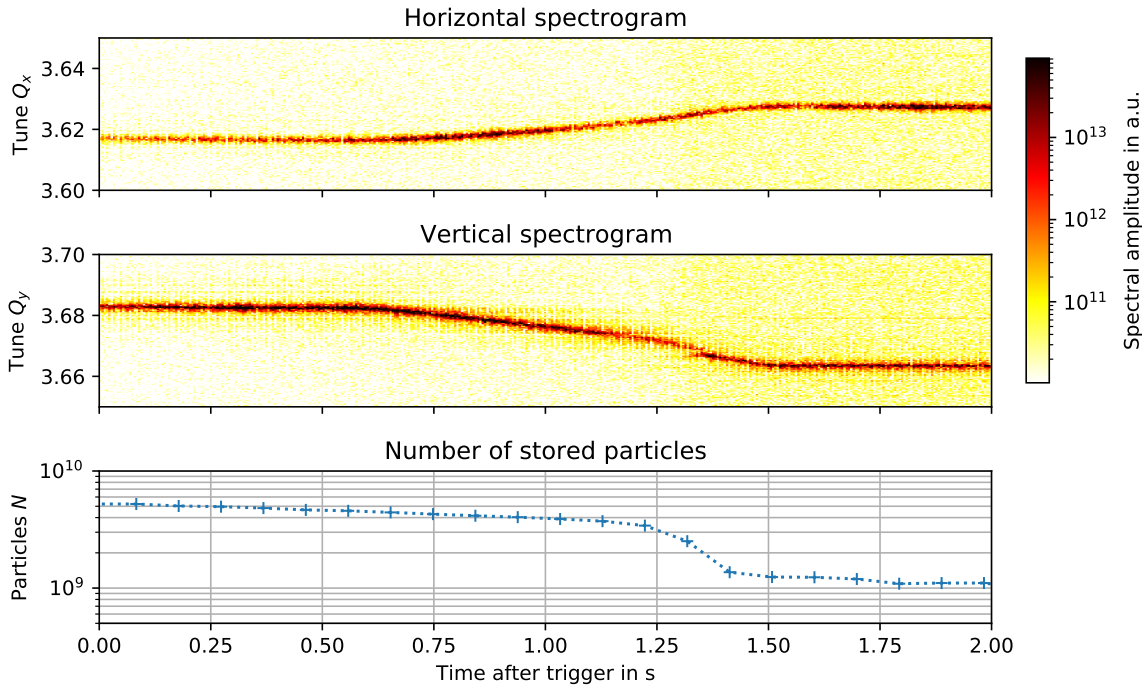

Figure 4.4.: Tune spectrogram over 2 s for a proton beam at $p = 521\,\mathrm{MeV}/c$. The visible tune change was caused by accelerating the beam by $0.6\,\mathrm{MeV}/c$ between 0.5 and 1.5 s after the trigger. The crossing of the vertical 2/3 resonance at $t = 1.3\,\mathrm{s}$ causes a significant beam loss (lower plot).

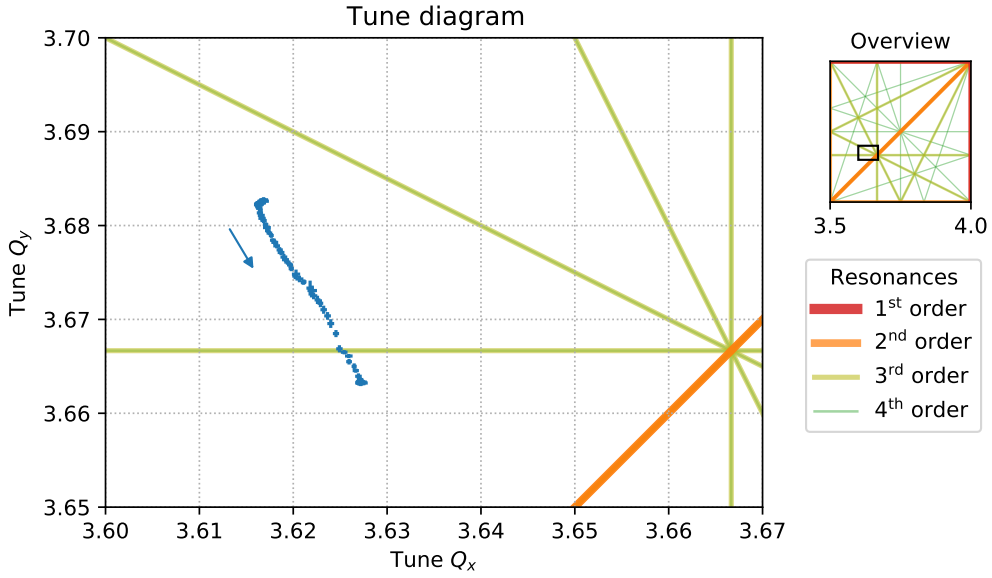

Figure 4.5.: Tune diagram for the measurement in figure 4.4. The arrow indicates the direction of time. While the horizontal tune increases, the vertical tune decreases and crosses the 2/3 resonance (yellow line).

Fourier transform (STFT): The data is divided into segments, each of which is Fourier transformed similarly to the ordinary tune measurement. This is implemented using the SciPy library [Opp99, pp. 714 sqq.; Sci].
The number of bunch positions per segment N_{seg} does not only determine the resolution in tune $\delta q = 1/N_{\text{seg}}$ as described above; It also determines the time resolution of the measurement: $\delta t = N_{\text{seg}}/f_{\text{rev}}$. Since the product $\delta q \cdot \delta t = 1/f_{\text{rev}}$ is fixed by the revolution frequency, a reasonable compromise has to be found. With $N_{\text{seg}} = 2^{10} = 1024$ at a typical frequency of $f_{\text{rev}} \approx 1\,\text{MHz}$ a resolution of three digits in tune and 1 ms in time can be achieved. This default value can be adjusted by the operator as needed for the specific application.

Figure 4.4 shows an exemplary tune spectrogram for both planes in which the tunes are clearly visible as bold lines. Each spectrum is fitted as described above, yielding the tune in its time evolution as visualized in the tune diagram (figure 4.5). For the given example, the tune change was induced by slightly increasing the beam momentum. Thereby, the vertical tune crosses the 2/3 resonance. The resulting beam loss is clearly visible as a reduction in the number of stored particles (lower plot of figure 4.4). However, the continuous excitation over several seconds itself also reduces the particle number from 5×10^9 to 4×10^9 over 1 s.
To reduce the excitation induced beam loss for continuous tune measurements, a pulse width modulation (PWM) is implemented to reduce the average excitation power. By specifying a duty cycle for the noise sample, a pulsed excitation can be achieved. As a result, the tune appears as a dashed line in the spectrograms, which also helps to clearly distinguish the tune resonance from other spurious signals.

The continuous tune measurement also provides the basis for the chromaticity measurement, which is discussed in chapter 5.

4.4. Integration into the COSY control system

At COSY the decentralised Experimental Physics and Industrial Control System (EPICS) [Epi] is used. Distributed Input / Output Controllers (IOCs) control hardware device, record data and perform online data analysis. They provide process variables (PVs) to receive data and modify parameters. These PVs can be accessed by clients over a dedicated protocol, called Channel Access (CA). This includes the graphical user interfaces (GUIs) in the control room, which are used to operate the accelerator, as well as the central data archiving system and automated scripts.

The routines for the excitation and tune measurement are implemented with the Python programming language. Therefore, the Python Device Support (PyDevSup) library [Mic] is used as a C based IOC implementation with an interface to Python. The developed EPICS IOC provides the PVs required for the tune measurement and calls the functions from the underlying Python implementation to communicate to

the hardware and perform the data analysis.

A dedicated GUI was developed to allow the operators to set up and configure the fast tune measurement system as well as to display the measurement results in a clear manner. The main interface (figure 4.7) allows to configure the beam excitation and measurement parameters. The operator can choose the BPMs to be used for the measurement from the list of available devices. By clicking on the respective labels, the frequency spectra and fits can be observed for each BPM (figure 4.8).
A tune diagram (figure 4.6) shows the current working point and up to five custom references. It includes the resonance lines to be avoided to support the operators in setting up and running the accelerator.
Screenshots of the GUI for the continuous tune measurement can be found in appendix B.2.
The documentation and operating manual for the developed measurement system is accessible via a "help" button. Additionally, the PVs were also registered in the central data archiving system and are thereby stored alongside other machine and measurement parameters.

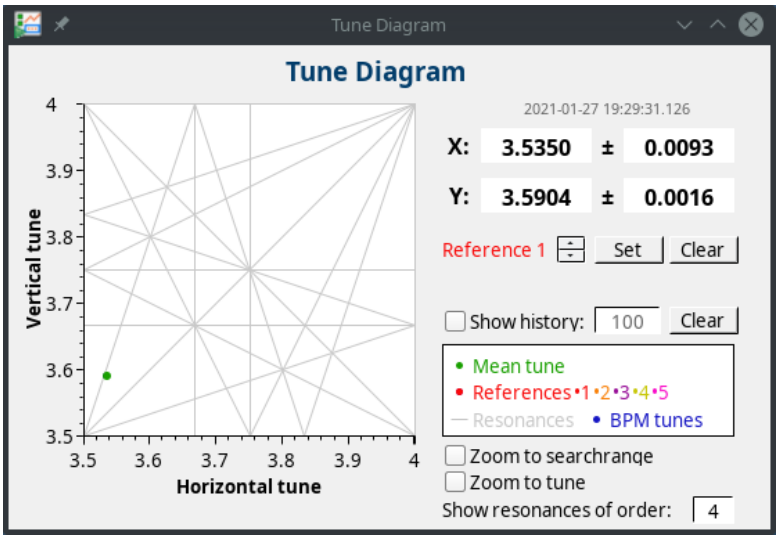

Figure 4.6.: Screenshot of the tune diagram in the fast tune GUI, showing resonances up to the 4^{th} order. The operator can set a number of references to compare different working points.

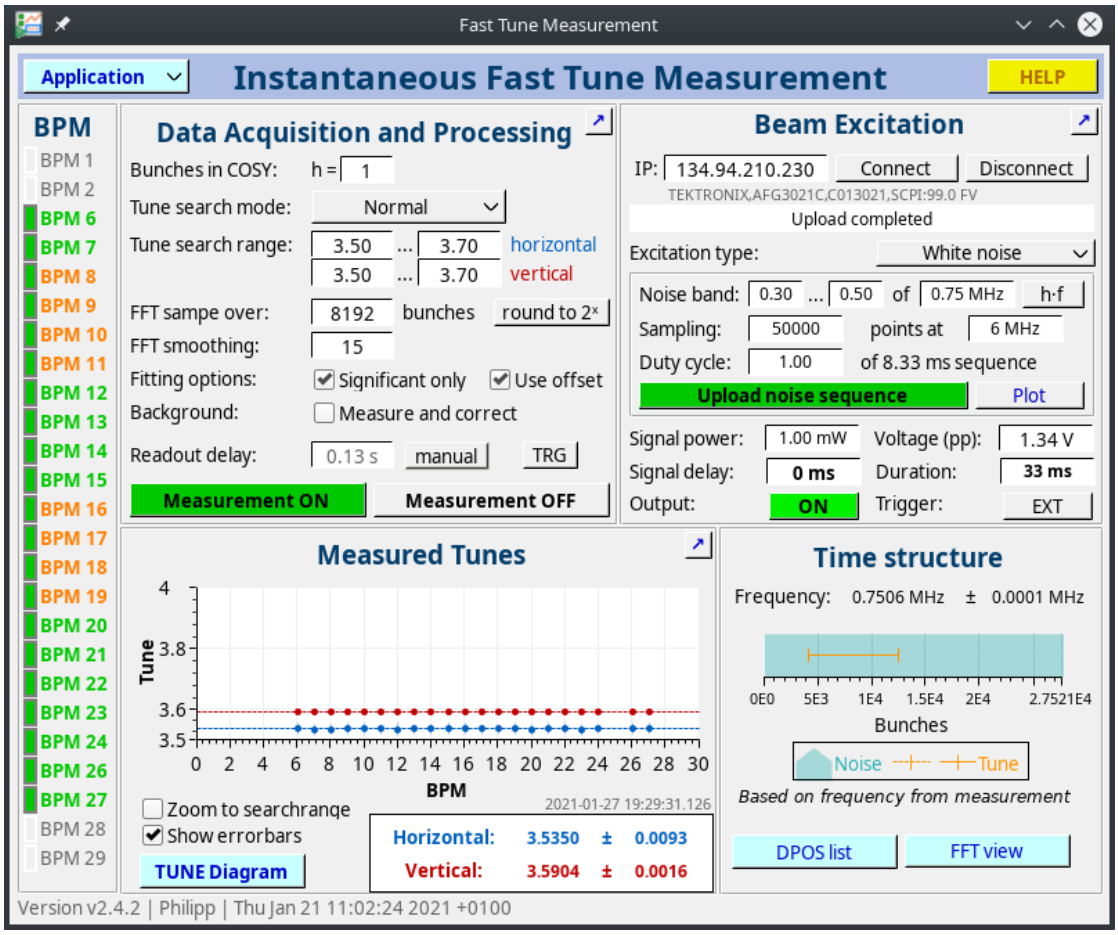

Figure 4.7.: Screenshot of the main fast tune GUI. Measurement options (upper left), beam excitation setup (upper right), measurement results (lower left) and time structure of the extracted subsamples (lower right).

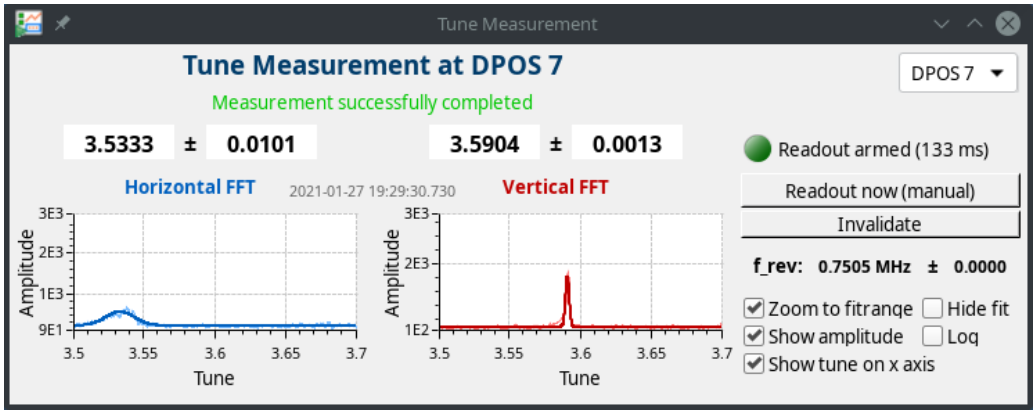

Figure 4.8.: Screenshot of a frequency spectrum of a single BPM in the fast tune GUI.

5. Development of a Chromaticity Measurement System

5.1. Measurement principle

The developed chromaticity measurement is based on the well established, classical method described in section 3.3.1, where a momentum change is induced and the subsequent tune change is measured. This method has the benefit that it can be built on top of the developed tune measurement. Since a measurement of the *total* chromaticity is envisaged, the momentum is changed via the revolution frequency while keeping the bending field constant.

Preliminary experiments with single tune measurements before and after jump-like momentum changes showed that multiple repetitions are required to achieve a sufficient measurement accuracy. Therefore, a slow but steady momentum change was chosen instead. This is realized by sweeping the RF frequency and continuously measuring the tune at the same time. By using a linear fit, the measurement accuracy is improved especially for small values of the chromaticity where the tune changes only slightly. This is particularly important for compensation of the chromaticity.

Using equation 3.3, the chromaticity is calculated from the linear change in revolution frequency and tune — both of which are derived from the bunch-by-bunch positions and timestamps. The only additional quantity required is the slip factor η, which can either be taken from a MAD model calculation or measured separately.

5.2. RF frequency sweep

In general, the frequency change — and therefore the momentum change — should be as large as possible to increase the sensitivity to small values of the chromaticity. However, the amplitude of the change is limited by several aspects:

- Since the linear chromaticity is to be measured, the change must be small enough such that the beam dynamics stay in the linear regime[1]
- A momentum change at fixed bending fields results in a dispersive orbit change, which has to be kept small in order to stay within the accelerator's acceptance

[1] In extension to the linear regime, a non-linear chromaticity can be defined, taking higher order tune changes into account [Wie15, p. 517]. See also section 6.4.2.

- If the change in tune is too large, the beam can become unstable as betatron resonances might be hit

According to [Ste09, p. 348], a relative momentum change $\Delta p/p$ in the range of 10^{-4} to 10^{-3} is to be favoured. The corresponding frequency change for a typical slip factor of $\eta \approx 0.6$ for COSY is in the sub-permille range. While preliminary tests showed non-linearities for larger frequency changes in the order of $\Delta f/f \approx \pm 1\,‰$, changes of about $\pm 0.3\,‰$ proved adequate.

The duration of the frequency sweep is chosen as a trade-off between excitation induced beam losses and a sufficient resolution in time for the linear regression. A sweep duration of about 0.5 s to 1 s was found to be adequate, longer sweep durations do not improve the measurement results but lead to an increased beam loss. Therefore, a symmetric frequency sweep of amplitude $0.6\,‰$ ($\pm 0.3\,‰$ with respect to the nominal frequency) and 1 s duration is suggested and used as default for the chromaticity measurement. In contrast to a unipolar asymmetric sweep, a bipolar symmetric sweep allows for a twice as large amplitude and is to be preferred.

At COSY, all synchronously ramped components are described as a function of time by piecewise polynomials. These are calculated prior to operation and stored in so called *fgen* files (see appendix B.1). The fgen files for the RF are loaded to a frequency generator, which outputs a variable sinusoidal signal according to the predefined frequency, phase and amplitude. After amplification, this signal is wave-guided to the RF cavity where the beam is bunched and accelerated.

For a chromaticity measurement, the bunched beam is temporarily accelerated by a precise linear frequency sweep. This is realized by adding corresponding linear segments to the fgen file. A dedicated script was developed to simplify the setup of the required frequency sweeps. This script reads the frequency fgen file and parses its contents. The polynomial at the specified cycle time is cut such that the sweep can be inserted. Given the sweep duration and its relative amplitude, three linear polynomials are added, creating a symmetric sweep as depicted in figure 5.1. The actual measurement takes place only during the rising flank. This process is repeated for each specified cycle time, allowing for multiple chromaticity measurements in a single machine cycle. Afterwards, the modified fgen file is saved and sent to the frequency generator as usual.

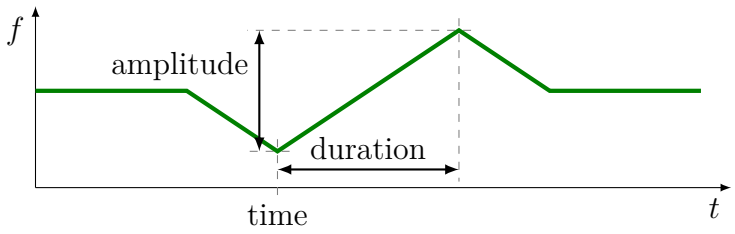

Figure 5.1.: Symmetric frequency sweep

5.3. Data analysis

For simplicity, the revolution frequency is reconstructed from the same bunch-by-bunch data that is being used for the tune determination. Therefore, the bunch timestamps provided by the Libera Hadron with a resolution of $\delta t = 4\,\mathrm{ns}$ are used. The revolution frequency can be determined with an accuracy of $\delta f/f = f\delta t \approx 4\,‰$ for a typical revolution frequency of $\mathcal{O}(1\,\mathrm{MHz})$. Since this is not sufficient for a chromaticity measurement, the resolution is increased by averaging over 1000 consecutive turns. This allows to resolve frequency changes down to 10^{-5} while still providing a time resolution of about 1 ms. The magnitude Δf of the frequency change can then be determined by a linear regression to the data.

The corresponding tune change is extracted from the spectrograms provided by the continuous tune measurement. Therefore, a two-dimensional fit is performed in the given tune search range and the time range of the linear frequency change. The scalar field fit function is:

$$A(q,\tilde{t}) = A_0 + A_1 \exp\left(-\frac{\left(q - q_0 - \Delta q \cdot \tilde{t}\right)^2}{2\sigma_\mathrm{q}^2}\right) \tag{5.1}$$

with the tune q, the normalized time $\tilde{t} \in [0,1]$ and the fit parameters A_0 (offset), A_1 (amplitude), q_0 (initial tune), $\Delta q = \Delta Q$ (tune change) and σ_q (tune spread). Since the amplitude of the spectrogram might vary over the measurement time, which can misguide the fitting algorithm, every spectrum is normalized to its maximum before applying the two-dimensional fit. Figure 5.2 shows an exemplary spectrogram for a chromaticity measurement (before normalisation) and the linear tune change from q_0 to $q_0 + \Delta q$ as determined by the two-dimensional fit.

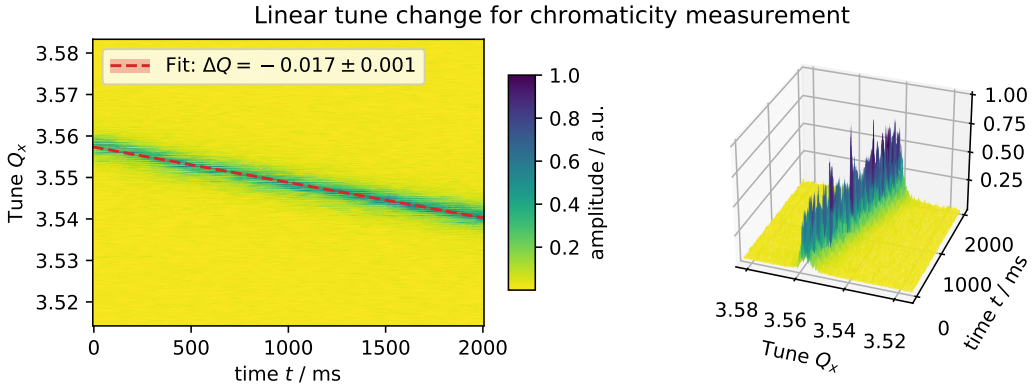

Figure 5.2.: Horizontal tune spectrogram for a chromaticity measurement of a cooled 970 MeV/c deuteron beam. The linear tune change was caused by a frequency change of +0.6 ‰ applied over 2 s. Therefore $\xi_x/\eta = -28.6(2)$.

The horizontal and vertical chromaticity $\xi_{x,y}$ is finally calculated from the relative frequency change and the tune change using equation 3.3. If the slip factor η is not known at the time of measurement (e.g. because it is measured afterwards), the ratio $\xi/\eta = \Delta Q/(\Delta f/f)$ is calculated instead.
For determination of the measurement uncertainty, not only the fit error is considered but also the tune resolution $\delta q = 1/N_{\text{seg}}$ (the pixel height in the spectrogram) by summation in quadrature. This prevents highly accurate fitting results from leading to a false precision beyond the true resolution, which is particularly important if the chromaticity is close to zero.

Considering a momentum change in the order of 10^{-4} to 10^{-3} as discussed in section 5.2, a tune resolution δq in the same order of magnitude is required to reach a resolution of one unit chromaticity. This can be achieved by computing the STFT on segments of 1000 to 10 000 bunch positions. Using a power of two, a default value of $N_{\text{seg}} = 2^{13} = 8192$ was chosen for the chromaticity measurements. With the product $\delta q \cdot \delta t = 1/f_{\text{rev}}$ fixed by the revolution frequency, the time resolution δt is typically in the order of 10 ms. Since a sufficient number of tune measurements is required for the linear regression, the time resolution gives a lower limit on the sweep duration as discussed in the previous section.

5.4. Integration into the COSY control system

The EPICS IOC and the corresponding GUIs for the tune measurement described in section 4.4 are extended with the readout and data analysis routines of the chromaticity measurement. The additional interface (figure 5.3) displays the frequency and tune change and the result of the linear fits. Together with the slip factor, the determined momentum change and chromaticity are shown.
Just as for the tune measurement, the data is archived centrally and the documentation and operating manuals are accessible via the “help” button.

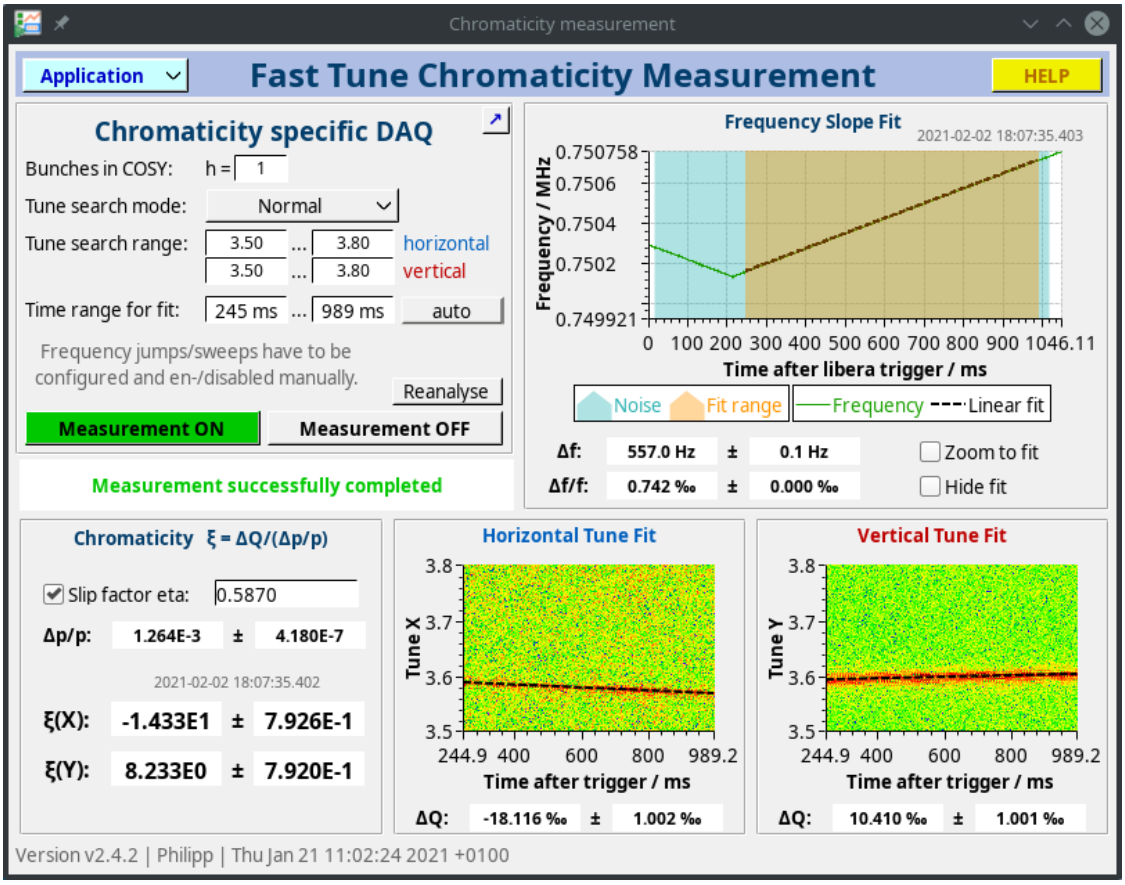

Figure 5.3.: Screenshot of the chromaticity measurement GUI

6. Commissioning and Measurements at COSY

6.1. Systematic study of tune signal strength

To determine the tune from the measured frequency spectra, the tune signal must be as large as possible such that it is clearly distinguishable from the background noise and any spurious signals. In this section the dependence of the tune signal strength is investigated with respect to the excitation power, the beam intensity, and the local amplitude of the betatron function at the BPM. To quantify the strength of the tune signal, the amplitude A of the Gaussian fit to the tune resonance peak in the frequency spectrum is chosen as observable. This amplitude does not include the background signal (offset).
The study is carried out with a deuteron beam at a momentum of $p = 970\,\mathrm{MeV/c}$ consisting of $1.60(3) \times 10^{10}$ deuterons stored in COSY. As can be seen in figure 6.1, the measured tune is $Q_x = 3.533 \pm 0.012$ and $Q_y = 3.590 \pm 0.002$. Since the horizontal tune is much wider, the amplitude is reduced compared to the vertical spectrum.

6.1.1. Dependence on excitation power

The dependence of the tune signal strength on the excitation power is studied. Therefore, the power of the noise excitation signal is systematically changed from 1 mW to 12 mW at the signal generator output. This corresponds to a range of 4 W to 48 W applied to the beam after amplification. For each measurement, the beam is excited over 33 ms with a noise signal in the frequency range of 0.3 to 0.5 times $f_{\mathrm{rev}} = 0.75\,\mathrm{MHz}$ ($h = 1$). The tune is then determined using an FFT over $2^{13} = 8192$ sampled bunch

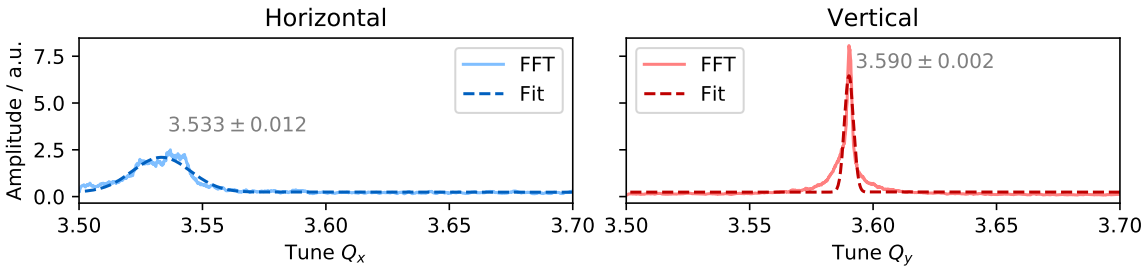

Figure 6.1.: Tune measurement for the excitation study

positions. For each setting of the excitation power, 15 measurements are performed to determine the average amplitude of the Gaussian fit as a measure for the strength of the tune resonance signal.

Figure 6.2 shows the measured dependency for three exemplary BPMs in the horizontal as well as vertical plane. The measured amplitude A scales with the square root of the excitation power P as

$$A(P) = p_0 \cdot \sqrt{P} + p_1 \tag{6.1}$$

The determined fit parameters p_i are listed in appendix C.1, where also additional plots for the other BPMs are given.
The square root dependency can be explained by the fact, that the average power of the excitation signal

$$P = \frac{1}{T} \int_0^T P(t)\,\mathrm{d}t = \frac{1}{T} \int_0^T \frac{U(t)^2}{Z}\,\mathrm{d}t \tag{6.2}$$

scales with the square of the signal voltage $U(t)$ where $P(t)$ is the instantaneous power, T is the signal duration and Z is the impedance of the stripline kicker the signal is applied to. The resulting oscillating electric field $E(t) \propto U(t)$ between the stripline electrodes drives the betatron oscillations. This process can be described by an ordinary harmonic oscillator driven by the force $F(t) = eE(t)$. The betatron

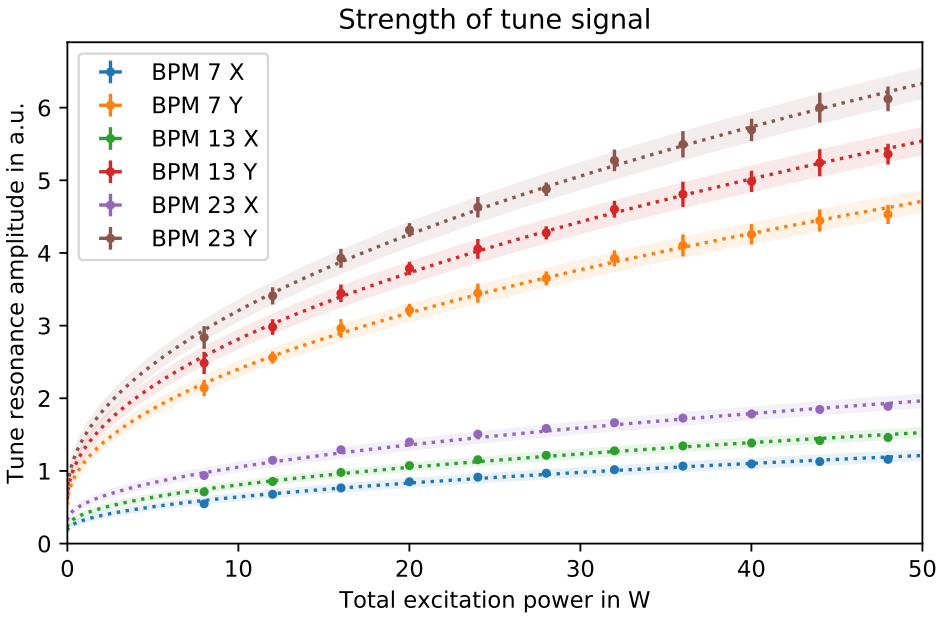

Figure 6.2.: Tune signal strength (amplitude of the Gaussian fit) in dependence of the excitation power. Fits are shown with a 1σ confidence interval.

oscillation amplitude increases until the exciting and damping forces compensate each other. In this steady state, the oscillation amplitude $\hat{x}$ of the harmonic oscillator is proportional to the driving force and therefore also proportional to the voltage $U \propto \sqrt{P}$. Hence, the measured dependency of the betatron oscillation amplitude agrees with the theoretical expectation $\hat{x} \propto \sqrt{P}$.

6.1.2. Dependence on betatron function

The amplitude of the tune resonance does not only depend on the excitation power but also varies significantly between different BPMs. If the amplitude scaling factor p_0 from the fits with equation 6.1 is plotted against the betatron function $\beta_{x,y}(s)$ at the location s of the respective BPM (figure 6.3), a strong correlation becomes visible. The values of the betatron function were calculated using a MAD simulation of the COSY lattice at the time of the measurement (see figure C.2 and tables C.1 and C.2 in the appendix). It has to be noted, that the simulation predicted a tune of $Q_1 = 3.613$ and $Q_2 = 3.695$ which is not in good agreement with the measured tune. This means that the betatron functions predicted by the MAD model are also imprecise. However, the deviation is expected to be negligible since the tune is the integral over the betatron function (equation 2.3) and therefore a small deviation in the betatron function results in a large deviation in tune.

Despite the model uncertainty, a clear square root like dependence of the amplitude

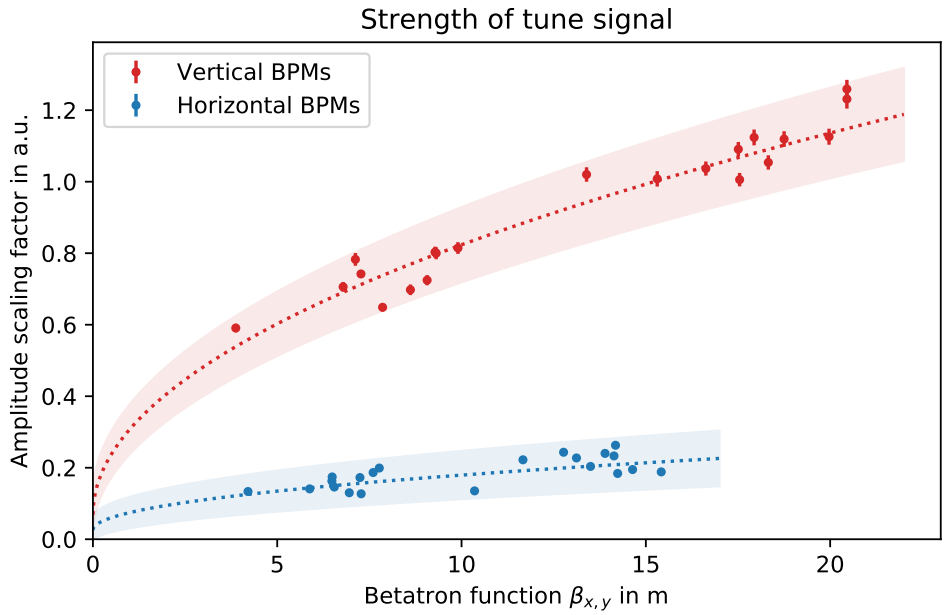

Figure 6.3.: Tune signal strength (scaling factor p_0) in dependence of the betatron function at each BPM based on a MAD model calculation.

scaling factor p_0 on the betatron function is found:

$$p_0(\beta_{x,y}) = b_0 \cdot \sqrt{\beta_{x,y}} + b_1 \tag{6.3}$$

The optimized fit parameters b_i for the horizontal and vertical plane are listed below. The parameter b_1 is negligible within the fit uncertainty.

Table 6.1.: Fit parameters for the tune signal strength dependence

	b_0 in a.u./$\sqrt{\text{Wm}}$	b_1 in a.u.
Vertical BPMs	0.239(17)	0.069(54)
Horizontal BPMs	0.048(11)	0.026(34)

The functional dependence is in agreement with the theoretical description (equation 2.2): the envelope of the betatron oscillation amplitude scales with $\hat{x} \propto \sqrt{\beta(s)}$. It is therefore preferable to perform the measurement using BPMs located at places with a large betatron function. For the machine settings presented here, BPM 8 is the best choice with $\beta_x = 15.42\,\text{m}$ and $\beta_y = 16.63\,\text{m}$. In addition, the BPMs 9, 17 and 22 have the largest betatron function in the vertical plane and the BPMs 8, 20 and 13 in the horizontal plane respectively (see tables C.1 and C.2).

6.1.3. Dependence on beam intensity

To investigate the influence of the beam intensity, the number of particles stored in COSY is varied by applying a PWM at the ion source ("micro-pulsing"). Thereby the excitation power is kept fixed at 48 W. For every setting of the beam intensity, the tune measurement is repeated at least 17 times (except for the lowest intensity where only 8 repetitions where made).

Figure 6.4 shows the result of the beam intensity study. In order to compare different BPMs, the measured amplitudes were normalized to the square-root of the betatron function. While the amplitude of the vertical tune resonance clearly increases with higher beam intensity, the amplitude in the horizontal plane stays about constant.
To discuss this behaviour, several aspects can be taken into account. In general, an increased number of particles draws more power from the exciting transverse field. However, this amount of power is negligibly small compared to the total excitation power even for 10^{11} particles, and therefore can not explain the observed dependence. A higher intensity also increases the sensitivity of the BPMs — especially since the signal amplification is constant — and thereby reduces the noise background. Therefore, one would expect an increase in the amplitude A. This is apparently not the case for the horizontal plane. The reason for this fundamental difference might be the distinct beam emittance, which is about 6 times larger in the horizontal plane.
To better understand this behaviour, further systematic studies are necessary to determine the effect of the beam emittance. Additionally, the influence of the BPM's

pre-amplifiers should be quantified independently in both planes.

In summary, the study shows that the tune measurement in the horizontal plane can not be improved by increasing the beam intensity, since this parameter only affects the vertical plane. However, choosing a large betatron amplitude and excitation power increases the signal amplitude in both planes and can therefore be used to improve the signal-to-noise ratio.

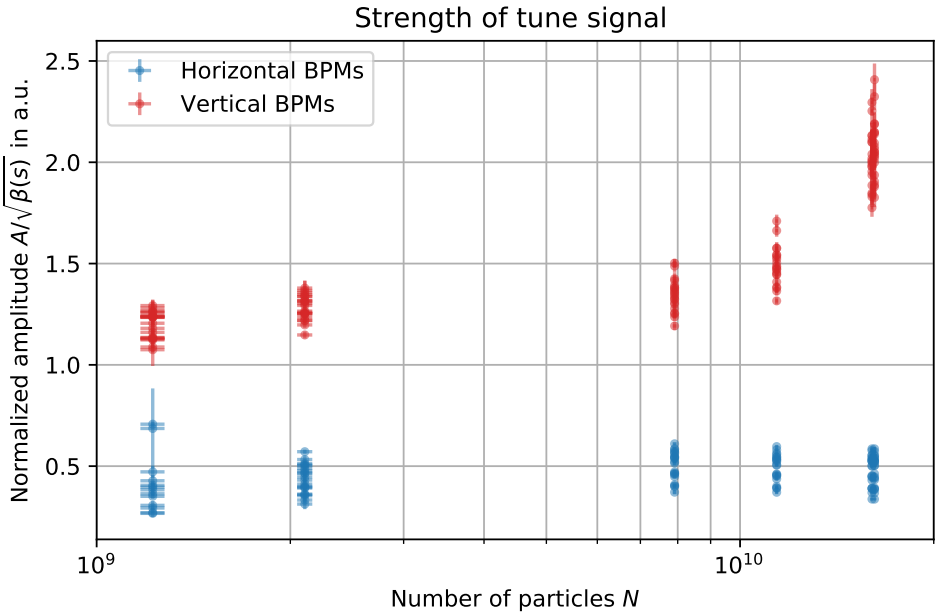

Figure 6.4.: Tune signal strength in dependence of the beam intensity. For each BPM, the amplitude A is normalized to the value of the betatron function $\beta(s)$ at the respective BPM.

6.2. Tune control with quadrupole magnets

For commissioning of the tune measurement system, the systematic adjustment of the working point using quadrupole magnets is demonstrated.

The lattice of COSY comprises a sixfold periodic ring structure and two straight telescopes (see figure C.3). Each telescope is equipped with four symmetric quadrupole triplets. A triplet consists of a focusing (F), a defocusing (D) and another focusing element, where the defocusing element needs to be twice as strong and is therefore realized with two magnets. With a phase advance of $\Delta\Psi = 2\pi$, the telescopes produce a 1:1 optical image, offering space for the beam cooling and diagnostic systems as well as internal experiments. [Bec86, pp. 7 sqq.; Hin08, pp. 184 sqq.]
The arcs are equipped with six mirror-symmetric FODO structures. The vertically focusing quadrupole magnets (F) are refereed to as MQU 1, 3 and 5; the horizontally focusing ones (vertically defocusing, D) are named MQU 2, 4 and 6. By adjusting the focusing strength k of these quadrupole groups, the tune can be controlled and set to the desired working point.

To adjust the tune, its dependence on the quadrupole strength is first quantified by measuring a tune response matrix. The determined matrix is then used to calculate the necessary settings for the quadrupole magnets in order to reach the desired working point. This is demonstrated in the following using a deuteron beam of 10^{10} particles at injection energy ($E_{\mathrm{kin}} = 55\,\mathrm{MeV}$, $p = 460\,\mathrm{MeV/c}$).

6.2.1. Measurement of the tune response matrix

The focusing strength k of a quadrupole magnet is proportional to the electric current I_{MQU} flowing through its windings. The relation between the current of the two quadrupole groups and the horizontal and vertical tune $Q_{x,y}$ can be described in linear approximation by the tune response matrix $\boldsymbol{M}$:

$$\begin{pmatrix}\Delta Q_x\\ \Delta Q_y\end{pmatrix} = \boldsymbol{M}\begin{pmatrix}\Delta I_{\mathrm{MQU\,1,3,5}}\\ \Delta I_{\mathrm{MQU\,2,4,6}}\end{pmatrix} \tag{6.4}$$

The tune response matrix is determined from tune measurements of at least three different quadrupole settings. Therefore, the system of linear equations obtained from the pairwise difference of each two measurements is solved. In the simplest case, three measurements are performed where only one of the two quadrupole groups is modified at a time. The linear system is then already diagonal, and the columns of the matrix can be calculated simply by dividing $\Delta Q/\Delta I$.
Figure 6.5 shows such a series of tune measurements for three different settings according to table C.3. From these measurements, the tune response matrix follows:

$$\boldsymbol{M} = \begin{bmatrix} -0.0294(50) & 0.0576(31)\\ 0.0709(21) & -0.0320(11)\end{bmatrix}\mathrm{1/A} \tag{6.5}$$

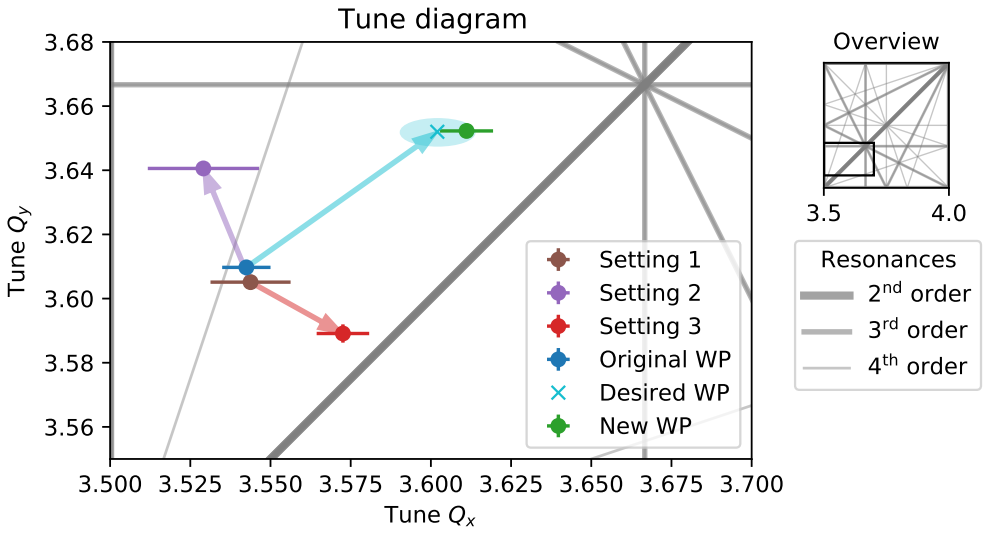

Figure 6.5.: Adjustment of the working point (WP) in the tune resonance diagram. Tune measurements for different settings of the quadrupole magnets are shown (purple: $\Delta I_{\mathrm{MQU\,1,3,5}} = 0.5\,\mathrm{A}$, red: $\Delta I_{\mathrm{MQU\,2,4,6}} = 0.5\,\mathrm{A}$). The linear tune shift is indicated with arrows and the uncertainty on the matrix calculation is marked with an ellipse.

Thereby, the uncertainty of the matrix is determined from the standard deviation of multiple tune measurements for each quadrupole setting using different BPMs.

6.2.2. Adjustment of the working point

The required quadrupole settings for a desired tune can be calculated from the original working point $(\vec{I}_{\mathrm{orig}}, \vec{Q}_{\mathrm{orig}})$ using the inverted tune response matrix $\boldsymbol{M}^{-1}$:

$$\begin{aligned} \begin{pmatrix} I_{\mathrm{MQU\,1,3,5}} \\ I_{\mathrm{MQU\,2,4,6}} \end{pmatrix} &= \vec{I}_{\mathrm{orig}} + \boldsymbol{M}^{-1} \left[\begin{pmatrix} Q_x \\ Q_y \end{pmatrix} - \vec{Q}_{\mathrm{orig}} \right] \\ \boldsymbol{M}^{-1} &= \begin{bmatrix} 10.2(10) & 18.3(12) \\ 22.6(19) & 9.4(22) \end{bmatrix} \mathrm{A} \end{aligned} \tag{6.6}$$

Using this equation, new quadrupole setting for a desired tune of $Q_x = 3.602$ and $Q_y = 3.652$ are calculated (table C.3). The original and desired working point are also shown in figure 6.5. An ellipse marks the area where the new working point is expected, considering the uncertainty of the measured tune response matrix. After applying the determined quadrupole settings, the new working point is measured to be $Q_x = 3.611 \pm 0.008$ and $Q_y = 3.652 \pm 0.001$. This corresponds to the desired working point within the expected uncertainty. Hence, the measurement and adjustment of the tune were demonstrated successfully.

6.3. Evolution of the tune during acceleration

In this section, the measurement of the tune evolution during acceleration of a deuteron beam to a momentum of $p = 970\,\mathrm{MeV/c}$ is demonstrated using the developed continuous tune measurement.
Figure 6.6 shows the tune in the horizontal and vertical spectrogram as well as the beam's momentum and revolution frequency for the complete acceleration ramp.
During the first 100 ms the previously unbunched (continuous) beam is bunched, which is reflected in the spectrograms by the narrowing tune signal. The beam is then accelerated by synchronously ramping up the frequency of the RF cavity and the fields of the magnets. While the tune — emerging as bold line in the spectrograms — changes only slightly throughout the ramp, one can also observe spurious signals that change rapidly. These interfere with the tune measurement especially in the horizontal plane. After about 1 s, the nominal momentum (flat top) is reached.

Since the noise used for excitation of the betatron oscillations has a fixed frequency band, this band has to be chosen appropriately such that the tune resonance is excited and visible throughout the whole measurement. Here, a frequency band of 0.3 to 0.5 times 750 kHz (flat top revolution frequency) was used. At the injection frequency

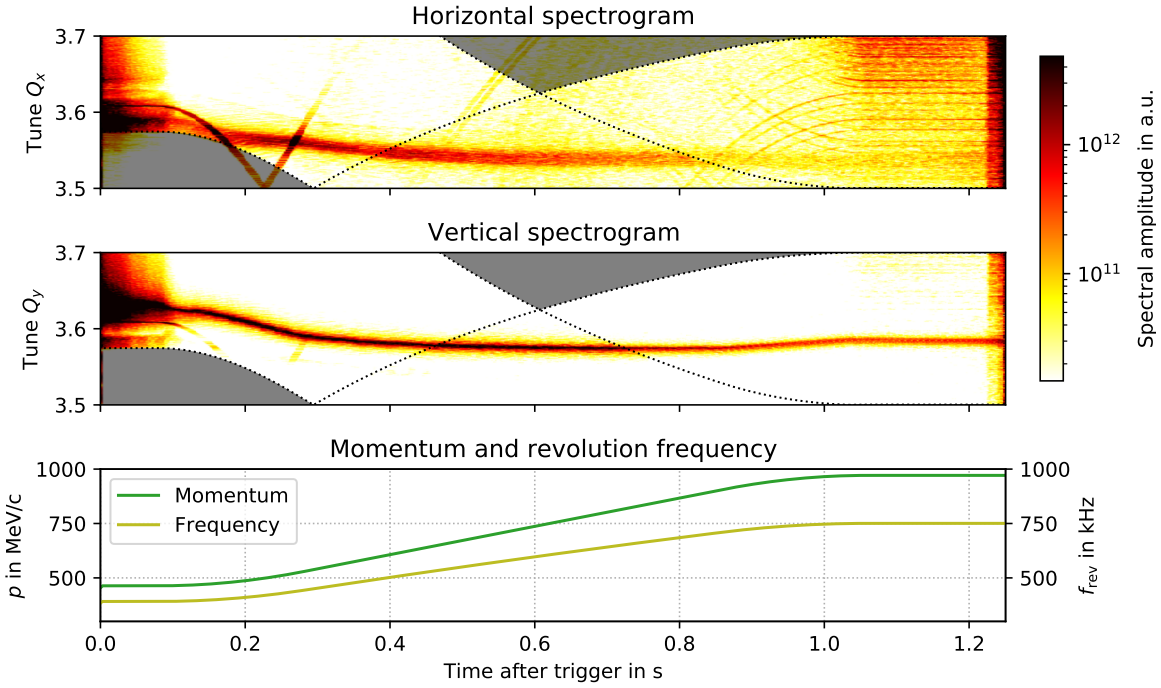

Figure 6.6.: Betatron tune during acceleration of a deuteron beam from 460 MeV/c to 970 MeV/c. The beam was excited with white noise in the range from 0.3 to 0.5 times 750 kHz, as indicated by the dotted lines (the mirrored band is also shown). Regions outside the excitation band are shaded.

($f_{\mathrm{rev}} = 392\,\mathrm{kHz}$), the relative excitation band is $f_{\mathrm{ex}}/f_{\mathrm{rev}} \in [0.57, 0.96]$. This leads to an excitation of the sideband below the first revolution harmonics at $f/f_{\mathrm{rev}} = 1 - r = Q - 3$ (compare section 3.2.2). As the beam is accelerated and the revolution frequency increases, the relative excitation band shifts to $f_{\mathrm{ex}}/f_{\mathrm{rev}} \in [0.3, 0.5]$, finally exciting the first sideband at $f/f_{\mathrm{rev}} = r = 4 - Q$. During the transition, these bands cross and partially overlap as indicated by the dotted lines in figure 6.6. This ensures a continuous excitation where only a small region (shaded) is not excited.
Especially in the horizontal spectrogram one can clearly see that the tune signal strength decreases throughout the measurement. The gradual decrease can be explained by the fact that the beam rigidity increases while the beam gains momentum, causing the excitation to be less effective. The significant drop at the dashed line near 0.8 s is caused by the betatron sideband at $1 - q$ leaving the excitation band. Since only the sideband at q remains excited, the spectral excitation power density is effectively halved.

In figure 6.7 the evolution of the betatron tune during the ramp is plotted in the tune resonance diagram. It is apparent, that the accuracy of the horizontal measurement is lower than the vertical one, as reflected by the larger uncertainties. This is because the fit is disturbed by the spurious signal at the beginning of the ramp and suffers from a reduced signal strength at the end of the ramp. Nevertheless, the transition from injection tune to flat top tune is clearly defined. The tune changes comparatively fast during the first 200 ms of the ramp, and then slowly until the nominal beam momentum is reached. Throughout the complete ramp, no resonance lines (up to the 4^{th} order) are crossed and the beam survives.

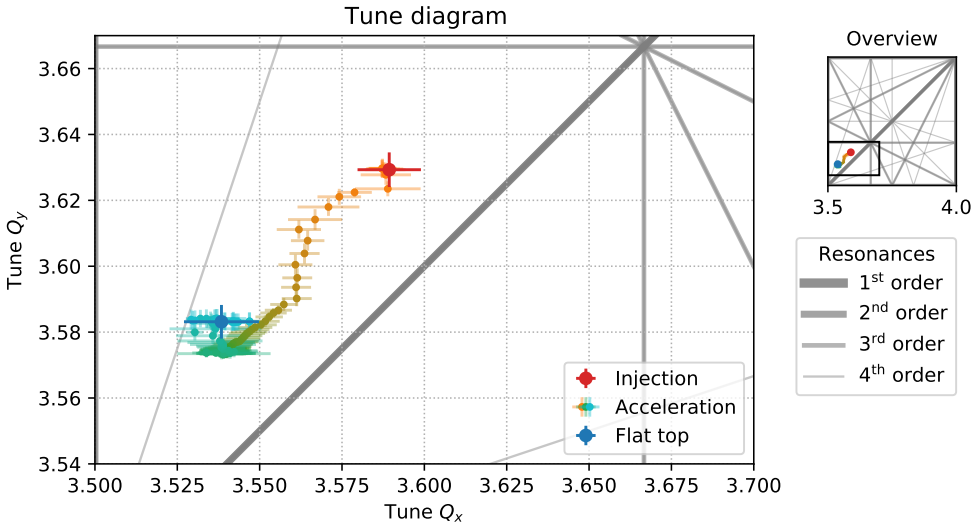

Figure 6.7.: Tune diagram corresponding to figure 6.6. The transition between injection tune ($Q_x = 3.589 \pm 0.010$, $Q_y = 3.629 \pm 0.006$) to flat top ($Q_x = 3.538 \pm 0.010$, $Q_y = 3.583 \pm 0.006$) is indicated by the colour gradient.

6.4. Chromaticity measurement and compensation

The chromaticity measurement system is commissioned using a machine configuration similar to the experimental setup used by the JEDI collaboration. A deuteron beam is accelerated to 970 MeV/c and cooled in all six dimensions of phase space using electron cooling. Thereby the momentum spread is reduced to $\Delta p/p = 1.4(2) \times 10^{-4}$. After the electron cooling is switched off with the electron cooler's solenoid remaining at its nominal field strength, 5×10^9 particles are stored in COSY for use by the experiment. The slip factor was measured to be $\eta = 0.533(1)$. The measurements presented in this section were carried out after the electron cooling but without prior orbit correction.

6.4.1. Measurement stability

The chromaticity measurement is tested with a positive symmetric frequency sweep of $\Delta f_{\mathrm{rev}}/f_{\mathrm{rev}} = 0.3\,‰$ amplitude over 2 s. The STFT is performed on segments of $N_{\mathrm{seg}} = 2^{13} = 8192$ consecutive position measurements. Figure 6.8 shows the measured linear tune change. The tune resonance peak in the spectrum is narrow due to the small momentum spread of the cooled beam. A comparison to a measurement without cooling is given in appendix C.3 where a much wider peak is observed. Even without cooling, the slope of the linear fit can be determined with high precision and the measured chromaticities agree within their uncertainties.

Furthermore, the duration, amplitude and polarity of the frequency sweep is varied to examine the stability and systematic uncertainty of the chromaticity measurement. Figure 6.9 shows the results of a number of measurements in subsequent machine cycles during which the properties of the frequency sweep were varied. The standard deviation of the measured values agrees with the uncertainty of a single chromaticity

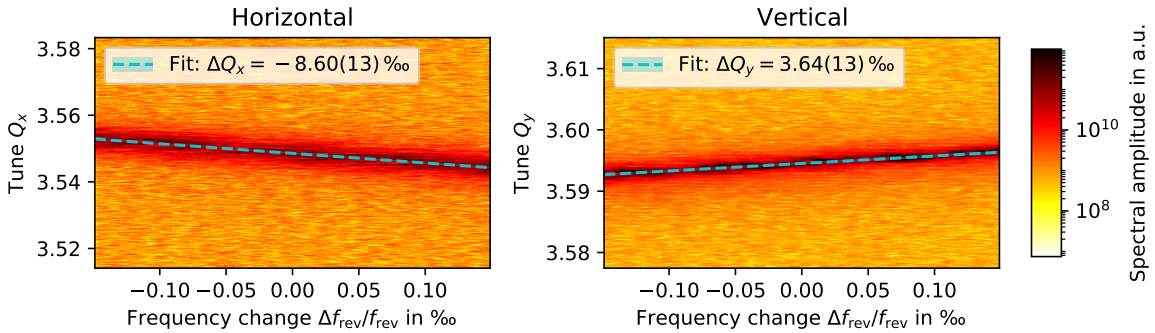

Figure 6.8.: Tune as function of frequency change for a chromaticity measurement of a cooled 970 MeV/c deuteron beam. The linear fit gives a frequency change of $\Delta f_{\mathrm{rev}}/f_{\mathrm{rev}} = 0.297\,76(4)\,‰$, a chromaticity of $\xi_x = -15.4(3)$, $\xi_y = 6.5(3)$ and a tune of $Q_x = 3.548\,56(14)$, $Q_y = 3.594\,53(14)$ at $\Delta f_{\mathrm{rev}}/f_{\mathrm{rev}} = 0$.

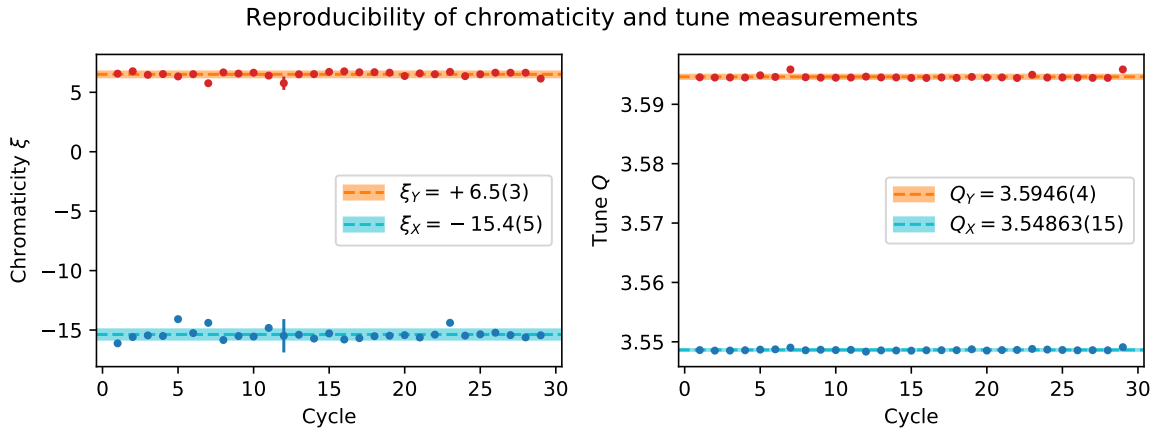

Figure 6.9.: Measured chromaticity (left) and tune (right) for frequency sweeps of different polarity, amplitude (0.3 ‰ to 0.6 ‰) and duration (1 s to 2 s). The average value and standard deviation is indicated.

measurement (figure 6.8), such that the reproducibility is confirmed.
By increasing the amplitude of the sweep by a factor of 2, the measurement uncertainty can be halved. On the other hand, an increased sweep duration does not improve the accuracy of the measurement.

6.4.2. Chromaticity compensation with sextupoles

As described in section 2.1.5, sextupole magnets can be used to adjust and compensate the chromaticity. This is demonstrated by comparing two measurements with and without compensation.
Figure 6.10 shows a chromaticity measurement with all sextupole magnets switched off. The observed tune change is dominantly linear and the determined chromaticity is comparatively large with a value of $\xi_x = -15.7(3)$ and $\xi_y = 7.43(3)$.
For the second measurement the sextupole magnets "MXG", which are located in the apexes of the COSY ring, are energized with 20 % of the maximum current. It is known from operational experience that this setting is suited to largely compensate the chromaticity. As can be seen in figure 6.11, the tune change is indeed smaller and the chromaticity is reduced to $\xi_x = -1.4(3)$ and $\xi_y = -1.13(9)$. Due to the small linear component, non-linear tune changes become apparent. These higher order terms are refereed to as non-linear chromaticity [Wie15, p. 517].

To quantify the non-linearity of the measurement, a polynomial of cubic degree is fitted to the data:

$$Q = Q_0 + \xi \cdot \frac{\Delta f_{\mathrm{rev}}}{\eta f_{\mathrm{rev}}} + \xi^{(2)} \cdot \left(\frac{\Delta f_{\mathrm{rev}}}{\eta f_{\mathrm{rev}}}\right)^2 + \xi^{(3)} \cdot \left(\frac{\Delta f_{\mathrm{rev}}}{\eta f_{\mathrm{rev}}}\right)^3 \tag{6.7}$$

with the tune Q_0 for zero momentum deviation, the chromaticity ξ, and the second and third order non-linear components $\xi^{(2)}$ and $\xi^{(3)}$ as fit parameters.

The optimized values of the non-linear fit parameters significantly depend on the degree of the polynomial. To quantify this effect, the degree was varied from 3 to 6 and the standard deviation of multiple fit results is used as systematic uncertainty. The resulting parameters and their total uncertainties for both measurements are given in table 6.2.

By comparing the linear fit component ξ of both measurements, it is apparent that the sextupole magnets indeed lead to a reduction of the chromaticity in both planes. It can also be seen, that the measured tunes were affected by the sextupoles. This is because the orbit was not corrected at the time of the measurement, such that the beam passed the sextupole fields off-centre. Therefore, the sextupoles have a non-zero focusing strength even for particles with vanishing momentum deviation, which leads to a shift in the tune.
The quadratic contribution to the chromaticity $\xi^{(2)}$ are only slightly affected by the sextupole fields. Only in the horizontal plane a difference larger than the uncertainty was measured, which might be explained by higher order components of the magnetic field. The cubic coefficients $\xi^{(3)}$ are all zero within the measurement uncertainty and therefore negligible.

In summary, the chromaticity measurement and the concept of chromaticity compensation with sextupole magnets were successfully demonstrated.

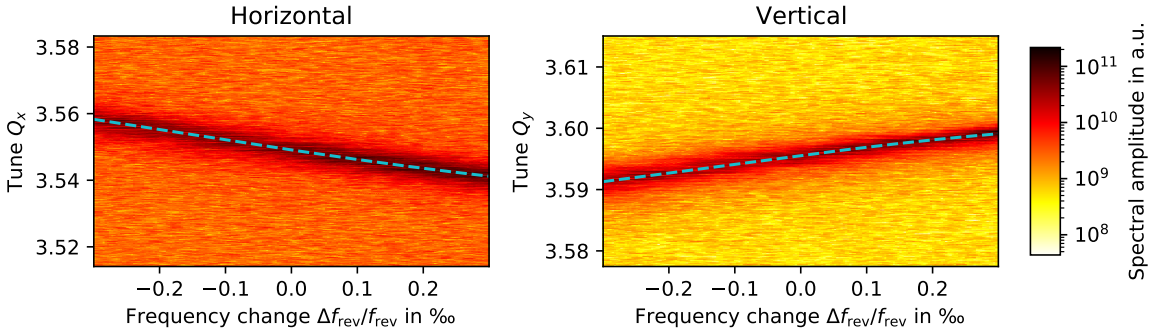

Figure 6.10.: Tune as function of frequency change for a chromaticity measurement with sextupole magnets switched off (uncompensated). The polynomial fit (dashed line) is dominated by the linear component.

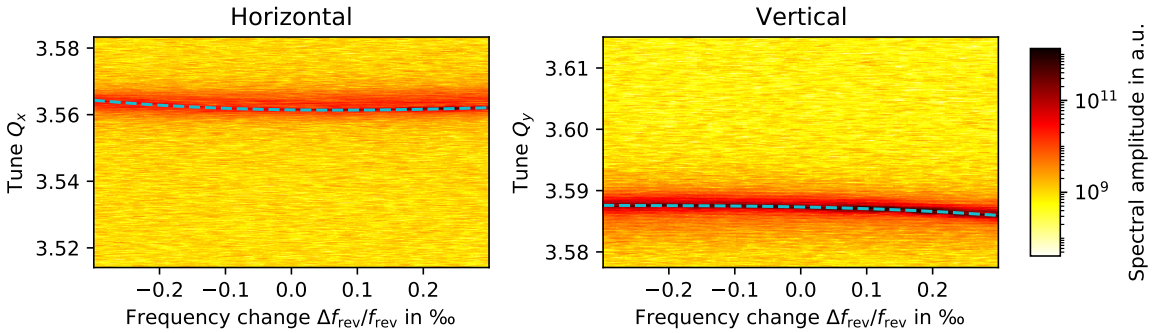

Figure 6.11.: Tune as function of frequency change for a chromaticity measurement with sextupole magnets switched on. The chromaticity is mostly compensated causing the linear component in the polynomial fit (dashed line) to vanish while higher order correlations become apparent.

Table 6.2.: Results for the cubic polynomial fits of the chromaticity measurements with and without compensation by sextupole magnets. Besides tune Q_0 and chromaticity ξ also the quadratic $\xi^{(2)}$ and cubic $\xi^{(3)}$ coefficients are given according to equation 6.7. The uncertainties in parentheses are the combined statistical and systematic uncertainties.

		Q_0	ξ	$\xi^{(2)}$	$\xi^{(3)}$
uncompensated	Hor.	3.549 10(3)	−15.7(3)	2.1(10) × 10^3	2(4) × 10^6
	Ver.	3.595 56(3)	7.43(3)	−1.1(7) × 10^3	−1.6(2) × 10^6
compensated	Hor.	3.561 44(3)	−1.4(3)	5.6(10) × 10^3	−2(4) × 10^6
	Ver.	3.587 34(3)	−1.13(9)	−1.8(13) × 10^3	−1.0(3) × 10^6

7. Conclusions

7.1. Summary

In the course of this thesis, a fast tune and chromaticity measurement system was developed and successfully commissioned. For excitation of the betatron oscillations via a stripline kicker, an adjustable, band limited noise source was implemented. The noise excitation allows for a short measurement time minimizing the impact on beam operation. It also enables continuous tracking of the tune independent of a changing revolution frequency.
The betatron tune is determined from bunch-by-bunch position measurements with capacitive pick-ups using the Libera Hadron beam position processor. Initiated upon a dedicated trigger, the tune is measured within about 30 ms with a resolution of at least 10^{-4}. The typical uncertainty achieved with this method is in the order of 10^{-3}, which also includes the tune spread.
If tracked continuously, the tune can be recorded as a function of time for up to 3 s. With the product of resolution in tune and time $\delta q \cdot \delta t = 1/f_{\mathrm{rev}} \approx 1\,\mu\mathrm{s}$ fixed by the revolution frequency, a 10 ms time resolution allows for 10^{-4} units in tune.
To measure the chromaticity, the tune is tracked with an increased resolution of 10^{-5} units in tune over 1 to 2 s. At the same time, the beam's momentum is varied with a symmetric linear sweep of the revolution frequency via the RF cavity. Using a relative change in frequency of $\pm 0.3\,‰$, the chromaticity is determined from linear fits to the tune and frequency change with a typical uncertainty of about 0.3 to 0.5 units.
For regular use during beam operation and experiments, the developed methods were integrated into the COSY control and data archiving system. Dedicated GUIs for setting up the measurement procedures and displaying of the results were designed and introduced to the operators during a training course.

Systematic parameter studies and measurements demonstrating the capabilities and limits of the systems were presented. These show that BPMs at locations with a large betatron function in the respective plane are to be used preferably for the measurement. Furthermore, the dependence of the tune signal strength on the excitation power was quantified and the influence of the beam intensity was examined.
Using the continuous tune tracking, it was shown how the crossing of a tune resonance causes a significant beam loss. Additionally, the tune evolution during the complete acceleration ramp of a deuteron beam was measured.
In the course of commissioning, the targeted adjustment of the betatron tune and control of the chromaticity were demonstrated. Based on a measured tune response

matrix, the tune is adjusted using quadrupole magnets. The chromaticity is compensated by sextuple magnets in the arcs of the COSY ring. Thereby, non-linear components in the chromatic behaviour where observed and quantified for a deuteron beam at a momentum of $p = 970\,\mathrm{MeV/c}$.
The systematic uncertainty of the measurement method was analysed. Both tune and chromaticity were found to be stable against variations in the measurement conditions within the stated measurement uncertainty.

The developed tune and chromaticity measurement systems are not only used during routine operation by the COSY operators, but also required for studies by the JEDI collaboration. They provide two of the many parameters necessary for the successful operation of an accelerator.

7.2. Outlook

The tune measurement is currently limited to bunched beams since it relies on beam position measurements. For unbunched beams, the tune can in principle be reconstructed from the unprocessed ADC data taken with the capacitive pick-ups. The feasibility of this approach has already been proven in the course of test measurements and can be implemented in the future.
The excitation of betatron oscillations using white noise turned out to be insufficient for high beam momenta $p \gg 1\,\mathrm{GeV/c}$. Therefore, an alternative excitation mode using a swept sinusoidal signal was implemented. While this allows to identify the tune in the frequency spectrograms at the time the excitation frequency is resonant (see appendix C.4), an online evaluation and fitting is still to be realised.

In addition to the tune measurement, one can also think of determining the phase advance at various BPMs by combining their measurements. While the noise excitation has the benefit of allowing for a short measurement time, the information on the betatron oscillation phase is blurred and difficult to obtain in an absolute manner. For this purpose, a sinusoidal excitation, as used in a BTF measurement or by a PLL tune tracker, is much better suited.
In the regular tune measurement, spurious signals are corrected by taking a background measurement without excitation. This approach is currently not used for continuous tune tracking because the background signal is in general not representative for the whole measurement period, especially since the revolution frequency might change. However, by pulsing the noise signal with a 50 % duty cycle, a repetitive background correction can be realized. As a side benefit, this will also reduce the impact of long excitations on the particle beam.

The online fit of the chromaticity measurement considers only the linear component as the primary objective of such a measurement. However, in some cases also the non-linear components of higher orders might be of interest, especially if the linear

chromaticity is close to zero as shown in section 6.4.2. For this reason, an option to quantify the non-linear chromaticity in the online measurement can be added to the software.
Another possible extension is the measurement of the *natural* chromaticity, which does not include the effect of sextupole field components. As described in section 3.3.1, this can be realized by changing the momentum via the dipole field strength rather than the revolution frequency. In contrast to the frequency, the information on the magnetic field change is not contained in the measured data, but can be extracted from the control system.

The HESR currently being build by the IKP for FAIR at GSI will also be equipped with the Libera Hadron beam position processors. This allows to adopt the developed tune and chromaticity measurement systems for use at the HESR as well. However, since FAIR uses the Front-end Software Architecture (FESA), the control system integration of the developed algorithms will have to be re-implemented for this purpose.

Bibliography

[Abu19] F. Abusaif et al. *Storage Ring to Search for Electric Dipole Moments of Charged Particles: Feasibility Study*. Tech. rep. CERN-PBC-REPORT-2019-002. CERN, 2019. arXiv: 1912.07881.

[And20] Achim Andres et al. *First electric dipole moment measurement of the deuteron with the waveguide RF Wien Filter*. Tech. rep. 2020. URL: http://www.ikp.fz-juelich.de/CBAC/documents/CBAC12/JEDI-2nd-Precursor-run_proposal_08.09.2020-cover.pdf (visited on Mar. 8, 2021).

[Bec86] U. Bechstedt et al. *Kühler Synchrotron COSY: Technische Beschreibung*. Vol. 370. Spezielle Berichte der Kernforschungsanlage Jülich. Jülich, 1986. URL: http://hdl.handle.net/2128/13529.

[Bet17] M. Betz et al. "Bunched-beam Schottky monitoring in the LHC". In: *Nuclear Instruments and Methods in Physics Research Section A: Accelerators, Spectrometers, Detectors and Associated Equipment* 874 (2017), pp. 113–126. DOI: 10.1016/j.nima.2017.08.045.

[Böh18] C. Böhme et al. "COSY Orbit Control Upgrade". In: *Proceedings of the 6th International Beam Instrumentation Conference (IBIC'17)* (Grand Rapids, MI, USA). JACoW, 2018, pp. 263–266. ISBN: 978-3-95450-192-2. DOI: 10.18429/JACoW-IBIC2017-TUPCF20.

[Bou95] Daniel Boussard. "Schottky noise and beam transfer function diagnostics". In: *CAS – CERN Accelerator School: 5th Advanced Accelerator Physics Course*. Geneva, 1995, pp. 749–782. ISBN: 92-9083-078-6. DOI: 10.5170/CERN-1995-006.749.

[Bre17] B. Breitkreutz et al. "Towards a new Tune Meter for COSY". In: *Institut für Kernphysik · COSY: Annual Report 2016 – Short Reports*. Ed. by Frank Goldenbaum et al. Berichte des Forschungszentrums Jülich. Jülich, 2017, p. 10. URL: https://www.fz-juelich.de/ikp/EN/Service/Download/Downloads/jahresbericht_2016_artikel.

[Brü20] Thomas Brückel and Thomas Gutberlet, eds. *Conceptual Design Report: Jülich High Brilliance Neutron Source (HBS)*. Vol. 8. Schriften des Forschungszentrums Jülich. Jülich, 2020. ISBN: 978-3-95806-501-7. URL: http://hdl.handle.net/2128/25874.

[Cas07] Maria Elena Castro Carballo. "Transverse Diagnostics For High Energy Hadron Colliders". PhD thesis. Universidade de Santiago de Compostela, 2007. URL: https://cds.cern.ch/record/1103499.

[Cas09] Friedhelm Caspers. "Schottky signals for longitudinal and transverse bunched-beam diagnostics". In: *CAS – CERN Accelerator School: Course on Beam Diagnostics*. Geneva, 2009, pp. 407–425. ISBN: 978-92-9083-333-8. DOI: 10.5170/CERN-2009-005.407.

[Coc98] D. Cocq et al. "The Measurement of Chromaticity via a Head-Tail Phase Shift". In: *Proceedings of the 8th Workshop on Beam Instrumentation (BIW'98)* (Stanford, USA). AIP Conference Proceedings 451, 1998, pp. 281–288. ISBN: 978-1-56396-794-8. DOI: 10.1063/1.57008.

[Coo65] James W. Cooley and John W. Tukey. "An algorithm for the machine calculation of complex Fourier series". In: *Mathematics of Computation* 19 (1965), pp. 297–301. DOI: 10.1090/S0025-5718-1965-0178586-1.

[Cos] IKP-4. *Large Scale Nuclear Physics Equipment: COSY*. URL: https://www.fz-juelich.de/ikp/ikp-4/EN/Forschung_2/Beschleuniger/_node.html (visited on Mar. 8, 2021).

[Die04] J. Dietrich et al. "Status of the Cooler Synchrotron COSY-Jülich and Future Plans". In: *Proceedings of the 19th Russian Accelerator Conference (RuPAC'04)* (Dubna, Russia). JACoW Publishing, 2004, pp. 6–8. URL: https://accelconf.web.cern.ch/r04/papers/tuai01.pdf.

[Die98] J. Dietrich and I. Mohos. "Broadband FFT method for betatron tune measurements in the acceleration ramp at COSY-Jülich". In: *Proceedings of the 8th Workshop on Beam Instrumentation (BIW'98)* (Stanford, USA). AIP Conference Proceedings 451, 1998, pp. 454–458. ISBN: 978-1-56396-794-8. DOI: 10.1063/1.57031.

[Epi] EPICS collaboration. *EPICS – Experimental Physics and Industrial Control System*. URL: https://epics-controls.org (visited on Mar. 8, 2021).

[Far04] F. J. M. Farley et al. "New method of measuring electric dipole moments in storage rings". In: *Physical review letters* 93.5 (2004), p. 052001. DOI: 10.1103/PhysRevLett.93.052001.

[Gas05] M. Gasior and R. Jones. *The principle and first results of betatron tune measurement by direct diode detection*. Tech. rep. LHC-Project-Report 853. Geneva: CERN, 2005. URL: https://cds.cern.ch/record/883298.

[Geb20] R. Gebel et al., eds. *Institut für Kernphysik · COSY: Annual Report 2019*. Vol. 4423. Berichte des Forschungszentrums Jülich. Jülich, 2020. URL: https://www.fz-juelich.de/ikp/DE/Service/Download/Downloads/jahresbericht_2019.

[Gri04] David J. Griffiths. *Introduction to elementary particles*. Weinheim: Wiley-VCH, 2004. ISBN: 978-0-471-60386-3. DOI: 10.1002/9783527618460.

[Gui18] G. Guidoboni et al. "Connection between zero chromaticity and long in-plane polarization lifetime in a magnetic storage ring". In: *Physical Review Accelerators and Beams* 21.2 (2018). DOI: 10.1103/PhysRevAccelBeams.21.024201.

[Hin08] Frank Hinterberger. *Physik der Teilchenbeschleuniger und Ionenoptik*. 2. Auflage. Berlin, Heidelberg: Springer Berlin Heidelberg, 2008. ISBN: 978-3-540-75281-3. DOI: 10.1007/978-3-540-75282-0.

[Ikp] IKP. *Nuclear Physics Institute*. URL: https://www.fz-juelich.de/ikp/EN/Home/home_node.html (visited on Mar. 8, 2021).

[Jed] JEDI Collaboration. *Jülich Electric Dipole moment Investigations: Introduction*. URL: http://collaborations.fz-juelich.de/ikp/jedi/about/introduction.shtml (visited on Mar. 8, 2021).

[Jon18] Rhodri Jones. "Measuring Tune, Chromaticity and Coupling". In: *Proceedings of the 2018 course on beam instrumentation for particle accelerators*. Geneva, 2018, pp. 240–258. arXiv: 2005.02753.

[Kam19] Vsevolod Kamerdzhiev et al. "BPM System Upgrade at COSY". In: *Proceedings of the 7th International Beam Instrumentation Conference (IBIC'18)* (Shanghai, China). JACoW Publishing, 2019, pp. 303–306. ISBN: 978-3-95450-201-1. DOI: 10.18429/JACoW-IBIC2018-TUPC04.

[Leh05] A. Lehrach et al. "Design Work for the High-Energy Storage Ring of the Future GSI Project". In: *Proceedings of the 2005 Particle Accelerator Conference (PAC'05)* (Knoxville, TN, USA). JACoW Publishing, 2005, pp. 776–778. ISBN: 0-7803-8859-3. DOI: 10.1109/PAC.2005.1590560.

[Mad] MAD. *Methodical Accelerator Design*. URL: http://cern.ch/mad (visited on Mar. 8, 2021).

[Mai90] R. Maier et al. "Non-Beam Disturbing Diagnostics at COSY-Jülich". In: *Proceedings of the 2nd European Particle Accelerator Conference (EPAC'90)* (Nice, France). JACoW Publishing, 1990, pp. 800–802. ISBN: 978-2-86332-090-7. URL: https://accelconf.web.cern.ch/e90/pdf/EPAC1990_0800.pdf.

[Mic] Michael Davidsaver. *EPICS Device Support in Python*. URL: https://github.com/mdavidsaver/pyDevSup (visited on Mar. 8, 2021).

[Num] The SciPy community. *Discrete Fourier Transform (numpy.fft) — NumPy v1.19 Manual*. URL: https://numpy.org/doc/stable/reference/routines.fft.html (visited on Mar. 8, 2021).

[Opp99] Alan V. Oppenheim, Ronald W. Schafer, and John R. Buck. *Discrete-time signal processing*. 2nd ed. Prentice Hall signal processing series. Upper Saddle River, NJ: Prentice Hall, 1999. ISBN: 978-0-13-083443-0.

[Plo18] Gerlind Plonka et al. *Numerical Fourier Analysis*. Cham: Springer International Publishing, 2018. ISBN: 978-3-030-04305-6. DOI: 10.1007/978-3-030-04306-3.

[Reh10] G. Rehm et al. "Measurement of Lattice Parameters Without Visible Disturbance to User Beam at Diamond Light Source". In: *Proceedings of the 14th Beam Instrumentation Workshop (BIW'10)* (Santa Fe, NM, USA). JACoW Publishing, 2010, pp. 44–48. URL: https://accelconf.web.cern.ch/BIW2010.

[San69] M. Sands. *The head-tail effect: An instability mechanism in storage rings*. Tech. rep. SLAC-TN-69-8. SLAC, 1969. URL: http://slac.stanford.edu/pubs/slactns/tn01/slac-tn-69-008.pdf.

[Sch97] Hermann Schmickler. "Diagnostics and Control of the Time Evolution of Beam Parameters". In: *Proceedings of the 3rd European Workshop on Beam Diagnostics and Instrumentation for Particle Accelerators (DIPAC'97)*. 1997, pp. 43–47. URL: https://cds.cern.ch/record/343809.

[Sci] The SciPy community. *A spectrogram with consecutive Fourier transform (scipy.signal.spectrogram) — SciPy v1.6.0 Reference Guide*. URL: https://docs.scipy.org/doc/scipy/reference/generated/scipy.signal.spectrogram.html (visited on Mar. 8, 2021).

[Sha92] Robert E. Shafer. "Beam position monitoring". In: *The Physics of Particle Accelerators Vol. I*. AIP Conference Proceedings 249. AIP, 1992, pp. 601–636. DOI: 10.1063/1.41980.

[Ste09] R. J. Steinhagen. "Tune and chromaticity diagnostics". In: *CAS – CERN Accelerator School: Course on Beam Diagnostics*. Geneva, 2009, pp. 317–359. ISBN: 978-92-9083-333-8. DOI: 10.5170/CERN-2009-005.317.

[Tan06] C. Y. Tan. "Tune tracking with a PLL in the Tevatron". In: *Nuclear Instruments and Methods in Physics Research Section A: Accelerators, Spectrometers, Detectors and Associated Equipment* 557.2 (2006), pp. 615–620. DOI: 10.1016/j.nima.2005.11.157.

[Wen18] Manfred Wendt. "BPM Systems: A brief Introduction to Beam Position Monitoring". In: *Proceedings of the 2018 course on beam instrumentation for particle accelerators*. Geneva, 2018, pp. 373–411. arXiv: 2005.14081.

[Wie15] Helmut Wiedemann. *Particle Accelerator Physics*. Cham: Springer International Publishing, 2015. ISBN: 978-3-319-18316-9. DOI: 10.1007/978-3-319-18317-6.

[Wil96] Klaus Wille. *Physik der Teilchenbeschleuniger und Synchrotronstrahlungsquellen: Eine Einführung*. 2., überarbeitete und erweiterte Auflage. Teubner Studienbücher Physik. Wiesbaden: Springer Fachmedien, 1996. ISBN: 978-3-519-13087-1. DOI: 10.1007/978-3-663-11039-2.

[Žni16] Matjaz Žnidarčič, Elvis Janezic, and Kevin Lang. "Beam Position Monitor for Circular Proton Accelerators". In: *Proceedings of the 7th International Particle Accelerator Conference (IPAC'16)* (Busan, Korea). JACoW Publishing, 2016, pp. 267–269. ISBN: 978-3-95450-147-2. DOI: 10.18429/JACoW-IPAC2016-MOPMR018.

The following publication related to this thesis is currently in preparation:

P. Niedermayer et al. "Development of a Fast Betatron Tune and Chromaticity Measurement System for COSY". Submitted to the *12th International Particle Accelerator Conference (IPAC'21)*.

Acknowledgement

Finally, I would like to thank all those who have supported me on my way to the completion of this work. Many thanks to Prof. Andreas Lehrach for introducing me to the topic and the valuable comments. I specially like to thank Bernd Breitkreutz for supervising my thesis, the extensive, inspiring and productive discussions and the support when I carried out measurements in the COSY control room. I also wish to thank my colleagues at the institute and especially my research group for the support, suggestions and the feedback on my work.

Appendix

A. Formula Derivations

A.1. Fourier transform of an amplitude modulated signal of periodic pulses

The Fourier transform of a signal $x(t)$ reads:

$$\mathcal{F}\{x(t)\}(f) = \frac{1}{2\pi} \int x(t) e^{-i2\pi ft} \, \mathrm{d}t$$

Consider a periodic signal of delta pulses with period length $T = 1/f_{\mathrm{rev}}$. The Fourier transform is given by [Jon18, p. 241]:

$$x(t) = \sum_n \delta(t - nT) \quad \Longrightarrow \quad \mathcal{F}\{x\}(f) = 2\pi f_{\mathrm{rev}} \sum_h \delta(f - hf_{\mathrm{rev}})$$

The spectrum consists of harmonics of the fundamental frequency at hf_{rev}.

Introducing an amplitude modulation by a harmonic oscillation of frequency f_q and amplitude $2a$, the modulated signal $\tilde{x}(t)$ can be expressed as:

$$\tilde{x}(t) = x(t)\left[1 + 2a\cos(2\pi f_q t)\right] = x(t)\left[1 + ae^{i2\pi f_q t} + ae^{-i2\pi f_q t}\right]$$

Using the linearity of the Fourier transform and that

$$\begin{aligned}
\mathcal{F}\left\{xe^{\pm i2\pi f_q t}\right\}(f) &= \frac{1}{2\pi} \int x(t) e^{\pm i2\pi f_q t} e^{-i2\pi ft} \, \mathrm{d}t \\
&= \frac{1}{2\pi} \int x(t) e^{-i2\pi (f \mp f_q)t} \, \mathrm{d}t \\
&= \mathcal{F}\{x\}(f \mp f_q)
\end{aligned}$$

the Fourier transform of the modulated signal finally reads:

$$\mathcal{F}\{\tilde{x}\}(f) = \mathcal{F}\{x\}(f) + a\mathcal{F}\{x\}(f + f_q) + a\mathcal{F}\{x\}(f - f_q)$$

where each harmonic of the fundamental frequency is now accompanied by two sidebands at $hf_{\mathrm{rev}} \pm f_q$. The magnitude of these sidebands scales with the modulation amplitude.

A.2. Momentum change for a B-field change at fixed revolution frequency

The relativistic momentum is given by $p = \gamma m v$ with $\gamma = 1/\sqrt{1-\beta^2}$ and $\beta = v/c$. Its derivative reads:

$$\frac{\mathrm{d}p}{\mathrm{d}v} = \gamma m + mv\frac{\mathrm{d}\gamma}{\mathrm{d}v} = \gamma m + mv\gamma^3\beta\frac{\mathrm{d}\beta}{\mathrm{d}v} = \gamma m\left(1+\gamma^2\beta^2\right) = m\gamma^3 \tag{A.1}$$

Therefore in linear approximation:

$$\frac{\Delta p}{p} = \frac{\mathrm{d}p}{\mathrm{d}v}\frac{\Delta v}{p} = m\gamma^3\frac{\Delta v}{\gamma m v} = \gamma^2\frac{\Delta v}{v} \tag{A.2}$$

At fixed revolution frequency f the change in the particle's velocity $v = fL$ depends only on the change in the orbit circumference L.

$$\mathrm{d}v = f\,\mathrm{d}L = \frac{v}{L}\,\mathrm{d}L \iff \frac{\Delta v}{v} = \frac{\Delta L}{L} \tag{A.3}$$

The change in circumference is determined by the change in the radius of curvature $R = p/(qB)$:

$$\mathrm{d}L = 2\pi\,\mathrm{d}R = \frac{2\pi}{q}\left(\frac{\mathrm{d}p}{B} - \frac{p\,\mathrm{d}B}{B^2}\right) = 2\pi R\left(\frac{\mathrm{d}p}{p} - \frac{\mathrm{d}B}{B}\right) \iff \frac{\Delta L}{L} = \underbrace{\frac{2\pi R}{L}}_{\alpha_\mathrm{p}}\left(\frac{\mathrm{d}p}{p} - \frac{\mathrm{d}B}{B}\right) \tag{A.4}$$

With the momentum compaction factor $\alpha_\mathrm{p} = 1/\gamma_\mathrm{tr}^2$ [Hin08, p. 237]. Using this relation and combining equations A.2 to A.4 one gets:

$$\frac{\Delta p}{p} = \gamma^2\frac{\Delta L}{L} = \frac{\gamma^2}{\gamma_\mathrm{tr}^2}\left(\frac{\Delta p}{p} - \frac{\Delta B}{B}\right) \tag{A.5}$$

Finally, the relation between a change in the magnetic bending field ΔB and the resulting momentum change Δp for a constant frequency follows:

$$\frac{\Delta p}{p} = \frac{1}{1-\gamma_\mathrm{tr}^2/\gamma^2}\frac{\Delta B}{B} \tag{A.6}$$

B. Implementation Details

B.1. Fgen file

Fgen files describe a property as a function of time by means of piecewise polynomials:

$$f(t) = \sum_n f_n(t) \quad ; \quad f_n(t) = \begin{cases} \sum_k p_{n,k} \left(t - t_n\right)^k & \text{if } t_n \le t < t_n + d_n \\ 0 & \text{otherwise} \end{cases} \quad ; \quad t_n = \sum_{i=0}^{n-1} d_i$$

where $f_n(t)$ is the n^{th} polynomial ($n = 1, 2, 3, \ldots$). Each polynomial is described by its duration d_n and N coefficients $p_{n,k}$ of order $k = 0, 1, 2, \ldots, N$. Since the polynomials are consecutive, each one starts at the time t_n according to the equation above where $d_0 = 0$ is the initial delay. At COSY, polynomials up to order $N = 3$ are used.
An exemplary fgen file for the revolution frequency is given in file B.1. In the fgen file, each line represents a polynomial encoded as colon-separated values. The first value is the polynomial's duration d_n in ms, and the following values are the coefficients $p_{n,k}$ from $k = 0$ to 3 in units of raw/ms$^{\text{k}}$. The conversion from raw units to the physical quantity depends on the device the fgen file is used for. For the RF, the conversion factor is 1/5.726 665 Hz/raw.

A typical frequency ramp consists of injection (*flat bottom*), acceleration (*ramp up*), time for experiments (*flat top*) and returning to the initial state (*ramp down*). For a chromaticity measurement during an experiment, a frequency sweep was added to the fgen file B.1. Therefore, the existing *flat top* polynomial was split (lines 11 and 15) and three linear segments were inserted (highlighted lines 12 to 14). The resulting function is depicted in figure B.1.

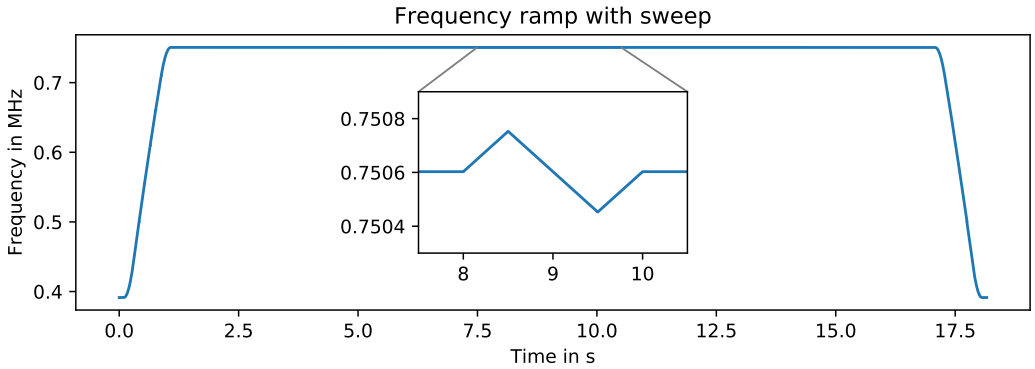

Figure B.1.: Frequency ramp according to file B.1. The inserted sweep is magnified.

File B.1.: `freq.fgen`

```
100:2241416.68:0.0:0.0:0.0
100:2241416.68:0.0:7.44602298:-0.000456312828
100:2315420.6:1475.51521:7.31312592:-0.00147264057
116:2534630.74:2893.96118:-0.39306158:-9.15271325e-05
116:2864898.33:2799.07613:-0.424903218:-7.06251239e-05
116:3183763.43:2697.64758:-0.449456704:-5.04615933e-05
116:3490563.89:2591.3366:-0.466982313:-3.15807519e-05
116:3784825.93:2481.72185:-0.477929778:-1.43828098e-05
100:4066252.19:2370.26153:-6.37820548:0.00180992911
100:4241306.22:1148.91831:-5.83510699:0.000603436279
6920:4298450.42:0.0:0.0:0.0
500:4298450.42:1.719380168000236:0.0:0.0
1000:4299310.110084:-1.719380168000236:0.0:0.0
500:4297590.729916:1.719380168000236:0.0:0.0
7080:4298450.42:0.0:0.0:0.0
100:4298450.42:0.0:-5.65407611:-0.000603436278
100:4241306.22:-1148.91831:-5.83522674:-0.00180992911
116:4066252.19:-2370.26153:-0.482934996:1.43828098e-05
116:3784825.93:-2481.72185:-0.477972415:3.15807518e-05
116:3490563.89:-2591.3366:-0.467017338:5.04615932e-05
116:3183763.43:-2697.64758:-0.449480761:7.06251239e-05
116:2864898.33:-2799.07613:-0.424913022:9.15271327e-05
100:2534630.74:-2893.96118:6.87133376:0.00147264057
100:2315420.6:-1475.51521:7.30912912:0.000456312829
100:2241416.68:0.0:0.0:0.0
end
```

B.2. Controls system GUI

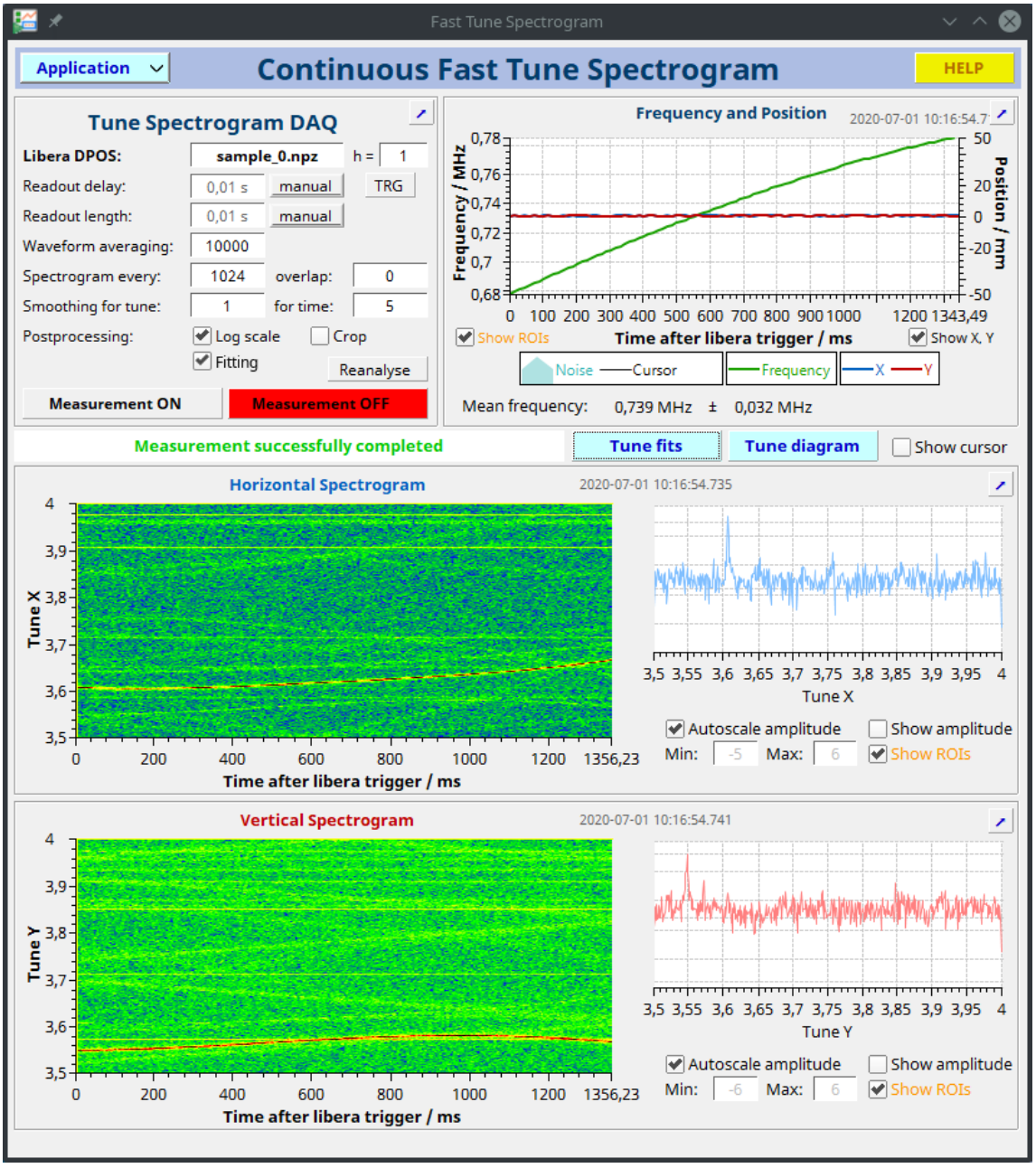

Figure B.2.: Screenshot of the continuous tune GUI allowing to configure the measurement parameters (upper left) and showing the frequency and beam position (upper right) and the tune spectrograms (coloured plots).

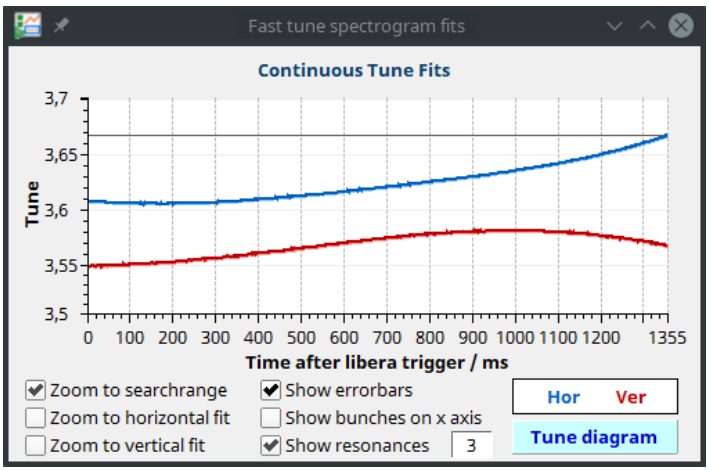

Figure B.3.: Screenshot of the continuous tune GUI showing the tune fits over time.

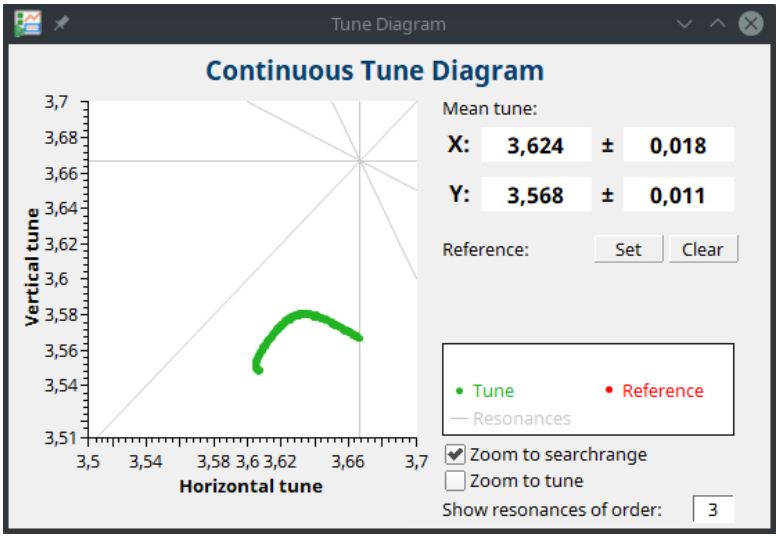

Figure B.4.: Screenshot of the continuous tune GUI showing the fitted tunes and their time evolution in the tune diagram.

C. Measurements

C.1. Excitation and tune signal strength

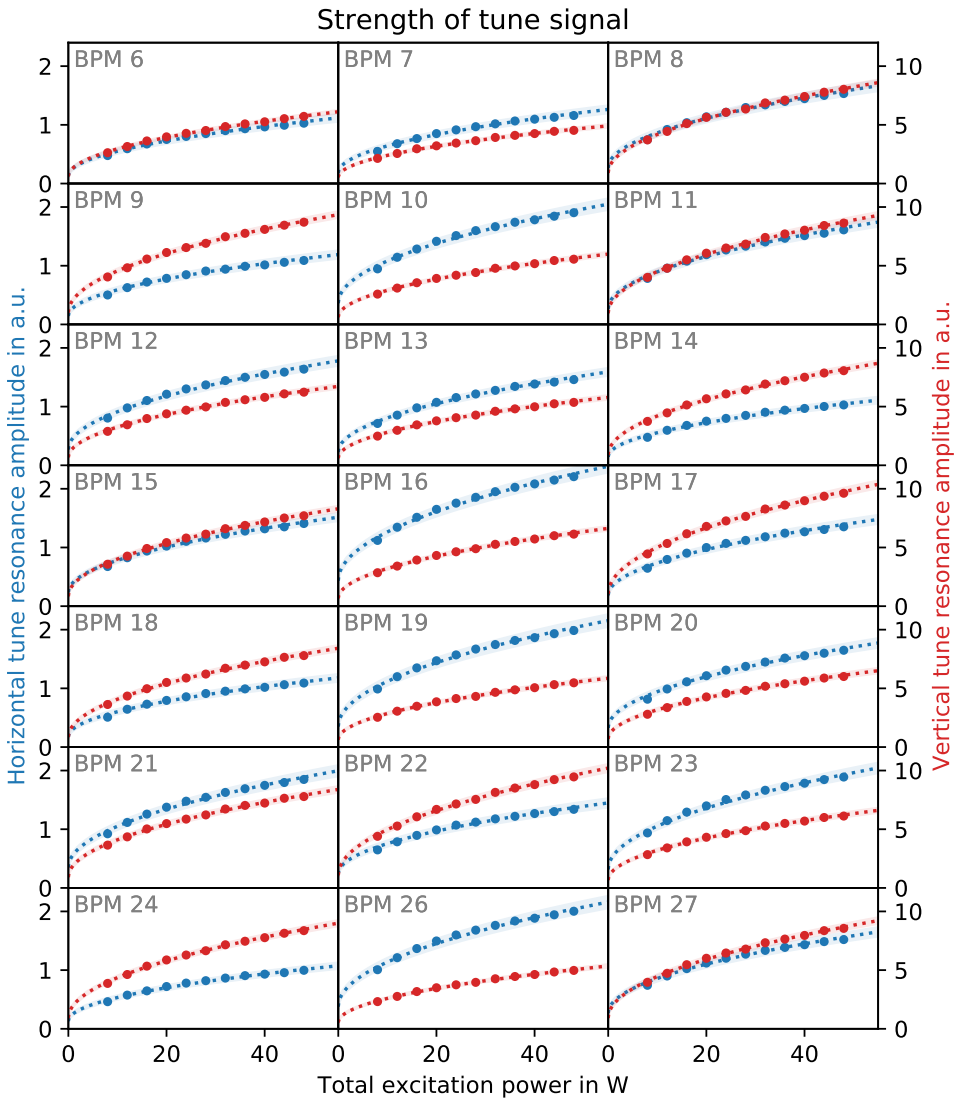

Figure C.1.: Amplitude A of the tune resonance as function of excitation power applied to the beam for different BPMs.

Table C.1.: Horizontal BPMs: Longitudinal coordinate s, betatron function β_x and fit parameters p_i for the square-root fits in figure C.1.

BPM	s in m	β_x in m	p_0 in a.u./$\sqrt{\text{W}}$	p_1 in a.u.
6 X	29.39	4.21	0.133(6)	0.129(27)
7 X	33.84	6.55	0.146(6)	0.181(28)
8 X	39.34	15.42	0.188(8)	0.269(38)
9 X	45.95	5.88	0.141(6)	0.145(29)
10 X	48.99	13.12	0.227(8)	0.362(40)
11 X	59.99	7.77	0.199(7)	0.267(33)
12 X	66.32	13.50	0.204(7)	0.269(34)
13 X	74.23	14.24	0.184(6)	0.227(27)
14 X	77.33	6.95	0.130(5)	0.145(25)
15 X	81.51	7.24	0.173(6)	0.236(28)
16 X	92.51	14.18	0.263(9)	0.434(44)
17 X	95.55	6.49	0.174(7)	0.186(31)
18 X	100.03	10.35	0.135(6)	0.175(28)
19 X	109.97	12.77	0.243(9)	0.350(45)
20 X	123.13	14.64	0.195(7)	0.328(34)
21 X	133.06	11.67	0.222(8)	0.348(40)
22 X	137.69	6.48	0.163(6)	0.240(33)
23 X	140.73	14.14	0.233(8)	0.316(36)
24 X	151.73	7.28	0.127(5)	0.132(23)
26 X	163.58	13.89	0.240(9)	0.378(43)
27 X	169.06	7.60	0.187(7)	0.269(33)

Table C.2.: Vertical BPMs: Longitudinal coordinate s, betatron function β_y and fit parameters p_i for the square-root fits in figure C.1.

BPM	s in m	β_y in m	p_0 in a.u./$\sqrt{\text{W}}$	p_1 in a.u.
6 Y	29.55	7.27	0.742(11)	0.614(57)
7 Y	33.99	3.88	0.591(12)	0.534(59)
8 Y	39.48	16.63	1.037(20)	0.906(103)
9 Y	46.10	19.97	1.126(23)	1.002(115)
10 Y	49.16	9.07	0.725(15)	0.618(73)
11 Y	60.15	17.94	1.124(23)	0.951(113)
12 Y	66.48	9.90	0.814(17)	0.683(84)
13 Y	74.40	8.61	0.698(15)	0.608(76)
14 Y	77.49	18.32	1.054(21)	0.874(102)
15 Y	81.35	17.54	1.006(19)	0.841(96)
16 Y	92.35	9.28	0.803(16)	0.672(78)
17 Y	95.40	20.45	1.259(26)	1.038(133)
18 Y	100.18	13.39	1.020(21)	0.852(103)
19 Y	110.12	6.79	0.706(14)	0.627(71)
20 Y	123.28	7.12	0.783(18)	0.700(90)
21 Y	133.22	15.31	1.008(22)	0.917(111)
22 Y	137.85	20.45	1.231(27)	1.079(135)
23 Y	140.89	9.31	0.800(17)	0.677(85)
24 Y	151.89	17.51	1.091(21)	0.911(104)
26 Y	163.43	7.86	0.649(12)	0.544(59)
27 Y	169.22	18.75	1.119(22)	0.917(112)

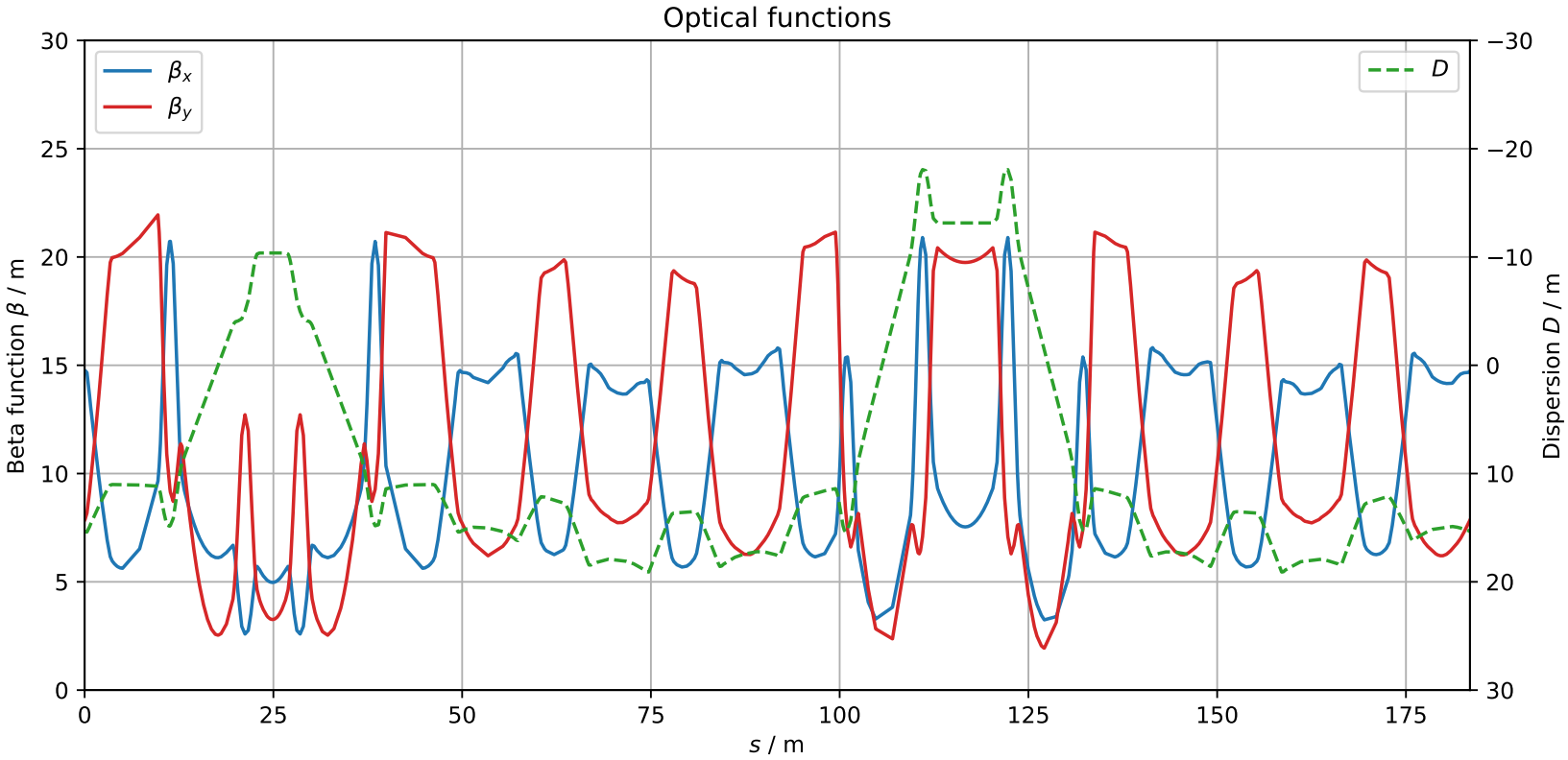

Figure C.2.: Optical functions of the COSY lattice: betatron function $\beta_{x,y}(s)$ and dispersion $D(s)$.

C.2. Tune adjustment with quadrupole magnets

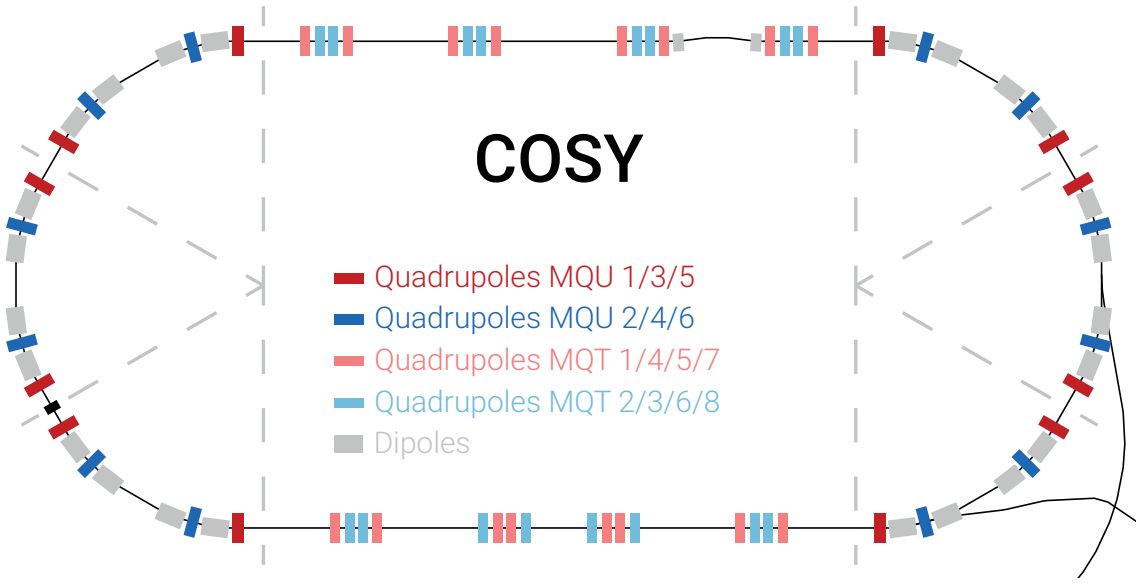

Figure C.3.: COSY lattice with quadrupole groups in the telescopes (MQT) and arcs (MQU). Horizontally focusing quadrupole magnets are shown in blue while vertically focusing ones are red.

Table C.3.: Tune measurements for different settings of the quadrupole magnets. For each setting, the tune Q averaged over 4 BPMs is listed with the standard deviation. Additionally, the measured tune spread σ_Q is given. The last two measurements where carried out one day later with a slightly different setting of dipole field and RF.

	$I_{\mathrm{MQU\,1,3,5}}$	$I_{\mathrm{MQU\,2,4,6}}$	Q_x	Q_y	σ_{Qx}	σ_{Qy}
Setting 1	24.90 A	34.10 A	3.5438(13)	3.6051(1)	±0.012	±0.002
Setting 2	25.40 A	34.10 A	3.5291(21)	3.6406(1)	±0.017	±0.002
Setting 3	24.90 A	34.60 A	3.5726(2)	3.5891(2)	±0.008	±0.003
Original WP	24.90 A	34.10 A	3.5425(5)	3.6097(1)	±0.008	±0.002
New WP	26.28 A	35.84 A	3.6111(3)	3.6523(1)	±0.008	±0.001

C.3. Tune and chromaticity measurements of a 970 MeV/c deuteron beam with and without beam cooling

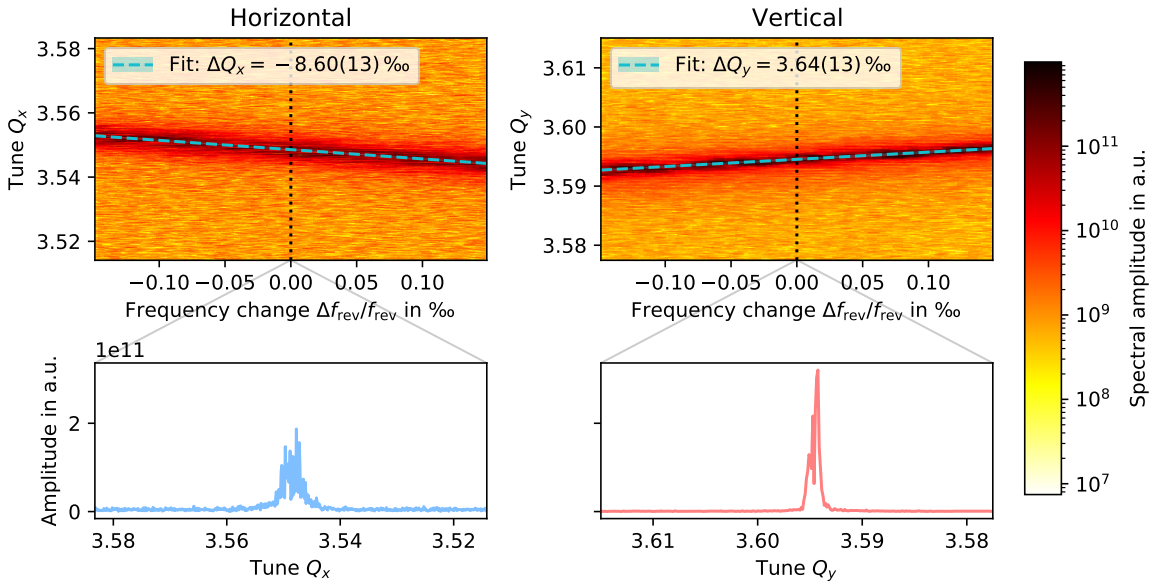

Figure C.4.: Chromaticity (top) and tune measurement (bottom) with pre-cooling: $\xi_x = -15.4(3)$, $\xi_y = 6.5(3)$, $Q_x = 3.548\,56(14)$, $Q_y = 3.594\,53(14)$

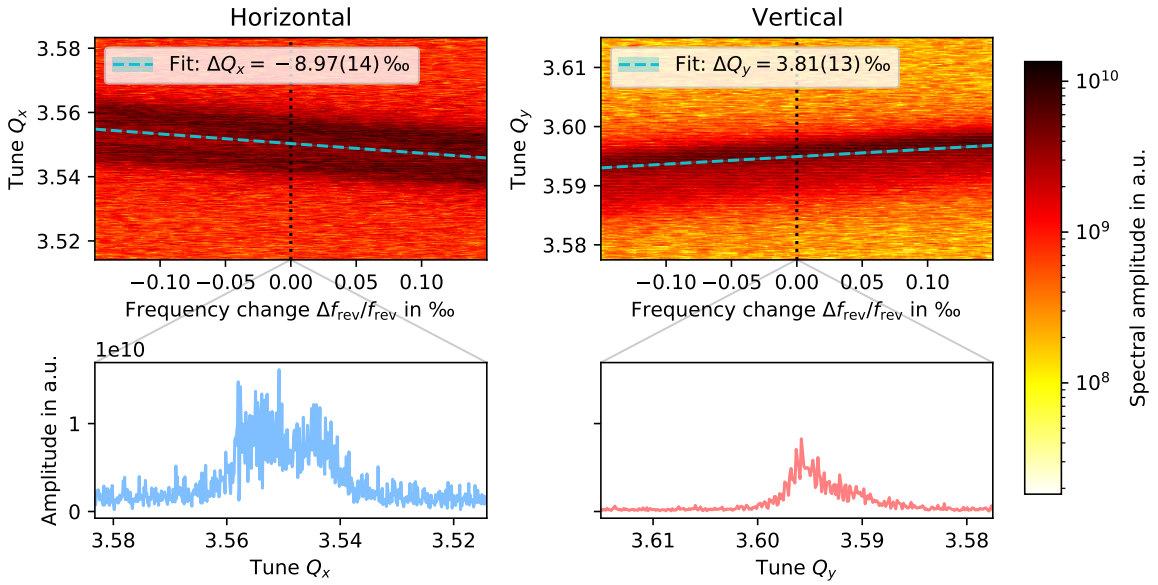

Figure C.5.: Chromaticity (top) and tune measurement (bottom) without cooling: $\xi_x = -15.9(3)$, $\xi_y = 6.8(3)$, $Q_x = 3.550\,32(15)$, $Q_y = 3.594\,92(14)$

C.4. Swept sinusoidal excitation

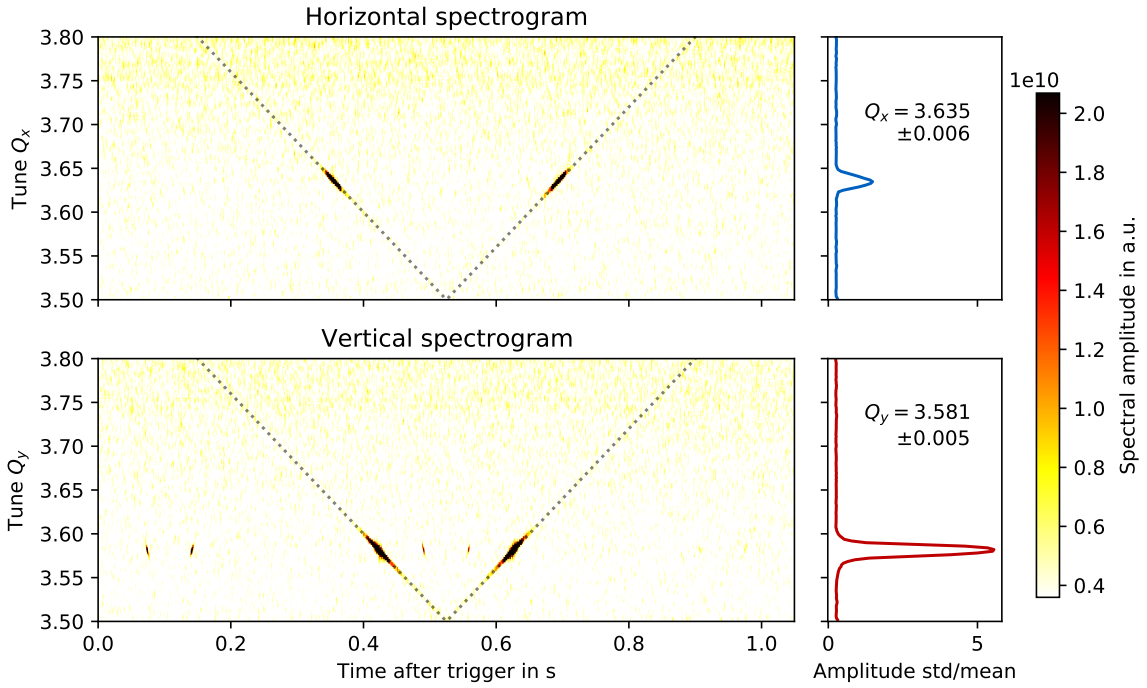

Figure C.6.: Frequency spectrograms recorded during excitation of the beam with a swept sinusoidal signal. The excitation frequency is swept from 0.1 to 0.9 times $f_{\mathrm{rev}} = 1.56\,\mathrm{MHz}$ during 1 s as indicated by the dotted grey lines. The tune manifests in the spectrograms by an increased spectral amplitude once it is crossed by the excitation frequency. The spectra on the right where added during offline analysis by calculating the standard deviation of the spectral amplitude for each row of pixels of the spectrogram, and dividing by the mean amplitude for this row. The spectra were fitted with a Gaussian, yielding $Q_x = 3.635 \pm 0.006$ and $Q_y = 3.581 \pm 0.005$